Journal of
Polymer Materials

Tech Science Press

http://doi.org/10.32604/jpm.2026.084491

ARTICLE

Chemical Surface Treatments of Luffa Fibers to Enhance the Interfacial Adhesion and Mechanical Properties of Unsaturated Polyester Composites

Ouided Dehas[1,2], Yasmina Biskri[1,2], Laidi Babouri[1,2], S. M. Anas[3,*], Osama Khan[4,*], Fouad Boukhelf[5,*], Aboulkacem Moutie Hamed[6] and Mohammed Benzerara[7,*]

[1]Higher Normal School of Technological Education of Skikda, Skikda, Algeria
[2]Laboratory of Anticorrosion-Materials, Environmental and Structure LAMES, University of 20 août 1955-Skikda, Skikda, Algeria
[3]Independent Researcher, New Delhi, India
[4]Department of Mechanical Engineering, College of Engineering, King Faisal University, Al-Ahsa 31982, Saudi Arabia
[5]Institut de Recherche de la Construction, ESTP-Grande Ecole d'ingénieurs de la Construction, 28 Avenue du Président Wilson, Cachan, France
[6]The Laboratory of Eco-Materials, Chemical Processes, and Sustainable Development, University of Biskra, Biskra, Algeria
[7]Materials Geomaterials and Environment Laboratory (LMGE), Department of Civil Engineering, Faculty of Technology, Badji Mokhtar-Annaba University, P.O. Box 12, Annaba 23000, Algeria
*Corresponding Authors: S. M. Anas. Email: mohdanas43@gmail.com; Osama Khan. Email: okhan@kfu.edu.sa; Fouad Boukhelf. Email: fboukhelf@estp.fr; Mohammed Benzerara. Email: mohammed.benzerara@univ-annaba.dz

Received: 23 April 2026; Accepted: 18 June 2026; Published: 24 September 2026

ABSTRACT: This study focuses on the reinforcement of thermosetting matrices with lignocellulosic fibers and the limited interfacial compatibility that remains a major obstacle to the structural use of bio-based composites. The effect of chemical surface treatment on the interfacial behavior and macroscopic performance of unsaturated polyester resin (UPR) reinforced with Luffa fibers (LF) is studied in depth. LF was treated with two different chemical treatments: (i) alkaline treatment with sodium hydroxide (NaOH) and (ii) a combined NaOH/acetic acid (CH_3COOH) treatment. The structural and morphological characteristics of the LF treated were examined using Fourier Transform Infrared Spectroscopy (FTIR) and Scanning Electron Microscopy (SEM). Composite specimens were fabricated through a contact molding technique. Mechanical performance was assessed via density, tensile strength, impact resistance, hardness test, and water absorption. Results demonstrate that composites containing 10 wt.% LF exhibits improvements in mechanical properties, with tensile strength, impact strength, and hardness increasing by 74%, 192%, and 16.2%, respectively. The chemical treatments further enhance performance by reducing water absorption and improving fiber–matrix interfacial densification. SEM observations indicate uniform fiber dispersion at low fiber contents, while higher loadings lead to fiber agglomeration. The results demonstrate that luffa fibers can serve as an eco-friendly strengthening material in unsaturated polyester resin composites.

KEYWORDS: Composites; vegetable fiber; luffa fiber; chemical treatment; unsaturated polyester resin; microstructure

1 Introduction

Polymers represent a significant part of our daily activities, with increasingly diverse applications [1,2]. The demand for these materials is continuously increasing due to their diverse physical and chemical properties, strong resistance to thermal variation, simple manufacturing processes, flexibility, and adaptability to different environmental conditions [3,4]. The use of reinforcing fillers in a polymer matrix makes it possible to obtain materials with improved or new properties, such as thermal, mechanical, electrical, and

optical properties. The main advantages of polymers include their ease of processing, high productivity, and cost-effectiveness [5,6].

In a wide range of uses, polymers are often enhanced by incorporating reinforcing materials to improve their strength and overall performance. Recent years have seen significant advances in research focused on thermosetting resin-based composite polymers reinforced with lignocellulosic fibers, such as sisal, hemp, banana, jute, and alfa [7–10]. Their main objective is to replace the glass and carbon fibers widely used by manufacturers in the production of sports equipment, containers, construction materials, automotive and aeronautical parts, etc. Industries are progressively turning toward plant-based fibers as they work to create greener technologies and eco-conscious materials. These fibers present benefits compared to artificial alternatives, including being lightweight, inexpensive, widely available, environmentally degradable, safe to handle, and possessing satisfactory strength and performance characteristics [11–13].

Many studies have explored the use of various reinforcing fibers in polymer composites [14–18]. Surface modification techniques have been employed to improve fiber–matrix adhesion [19–23]. Other investigations have focused on hybrid reinforcement strategies and particulate fillers [24–28]. Recent studies have reported the effectiveness of natural and sustainable fibers for enhancing composite performance [29–33]. Additional work has examined the durability and long-term behavior of these materials [34–36].

Baghloul et al. [37] found that adding marble waste (10–15% by weight) to a polyester resin improves mechanical properties and thermal stability due to enhanced matrix-filler interaction. However, higher contents (~20%) lead to a decline in performance due to particle agglomeration and microstructural defects. Dehas et al. [38] investigated the development of composites based on UPR reinforced with recycled PET fibers derived from post-consumer bottles. Their results show that incorporating low levels (5 to 8%) of long fibers (15 mm) improves mechanical properties, particularly tensile strength and impact resistance, due to good dispersion and strong fiber-matrix adhesion. However, higher fiber contents lead to fiber entanglement and a decrease in performance.

Luffa fibers (LF) present distinctive structural and functional characteristics that differentiate them from conventional lignocellulosic reinforcements. Unlike dense fibers such as jute or sisal, luffa exhibits a naturally interconnected three-dimensional porous network composed of aligned fibrous bundles and internal channels, which contribute to low-density, high-energy absorption capacity, and enhanced specific mechanical properties. This hierarchical architecture is particularly advantageous for lightweight composite applications and facilitates resin impregnation at low fiber contents. However, this same porous structure also increases susceptibility to moisture uptake and interfacial defects, making luffa fibers an excellent model system for studying the relationship between microstructure, interfacial behavior, and composite performance. Recent studies have highlighted the potential of luffa fibers in polymer composites, while emphasizing the need for optimized surface treatments to overcome their inherent hydrophilicity and improve compatibility with hydrophobic matrices [39–41].

Experimental studies on hybrid architectures (plant fibers combined with synthetic fibers such as fiberglass or Kevlar) have reported significant improvements in mechanical performance and reduced water absorption when alkaline pretreatments are applied, highlighting the critical role of fiber surface modification in composite performance [13]. Similarly, studies on natural fibers such as jute, sisal, banana, palm, and oil palm have demonstrated that their high moisture sensitivity and interfacial incompatibility with hydrophobic polymer matrices are mainly associated with the presence of hemicellulose, lignin, waxes, and abundant hydroxyl groups on the fiber surface [17,22,28–30,32]. These limitations are also relevant for luffa fibers and motivate the use of chemical surface treatments. In particular, alkaline treatment can remove amorphous non-cellulosic constituents and increase surface roughness, while subsequent acetic

acid treatment may partially modify accessible hydroxyl groups, thereby reducing fiber hydrophilicity and improving fiber–matrix interfacial adhesion. Such modifications are expected to enhance both the durability and mechanical performance of UPR/LF composites.

The improvement of the fiber-matrix interface through chemical treatments (NaOH, acetylation, silanization) and matrix modification (functional agents, nanoscale fillers) is a major methodological focus. Earlier research indicates that removing contaminants, enhancing the texture of the fiber surface, and applying bonding agents lead to stronger bonding at the interface [17,20,22]. This, in turn, results in better mechanical performance, such as higher tensile and flexural strength, improved impact durability, as well as reduced moisture uptake. The introduction of nanofillers or nanofibers is also reported to be an effective strategy for increasing toughness and limiting crack propagation (Mode I), provided that dispersion and the interface are controlled [14,24]. As regards modeling/diagnostics, micromechanical approaches that consider interfacial debonding and temperature dependence now make it possible to better predict structural properties and sensitivity to operating conditions, thus complementing experimental investigations [15,18].

The interfacial incompatibility between natural fibers and polymer matrices is primarily governed by the chemical composition of lignocellulosic fibers. These fibers are mainly composed of cellulose, hemicellulose, lignin, and surface extractives such as waxes and pectins. Among these constituents, hemicellulose and lignin contribute to the hydrophilic nature of the fibers due to the abundance of hydroxyl (–OH) functional groups, which promote moisture absorption and weak interfacial bonding with hydrophobic polymer matrices such as unsaturated polyester [42,43]. In addition, surface impurities and waxy layers hinder effective stress transfer by limiting direct contact between the fiber and the matrix. As a result, the presence of these components leads to poor adhesion, increased porosity at the interface, and reduced mechanical performance. Therefore, chemical surface modification strategies are essential to tailor fiber surface chemistry, reduce polarity, and enhance interfacial compatibility in bio-composites [39,44].

Despite this progress, several obstacles remain and justify a specific study of Luffa cylindrica. The literature shows that the effectiveness of treatments depends heavily on the operating parameters and the specific morphology of each fiber, and that the detailed correlation between microstructure (dispersion, agglomeration, surface topography) and mechanical/hygro-mechanical behavior remains incomplete [17,24]. Furthermore, although practical cases of industrial integration (nonwovens, automotive components) have been presented for certain fibers, process standardization and long-term evaluation (durability, aging, abrasive wear) remain challenges for widespread adoption [32,35,36].

Several studies have reported excellent mechanical and thermal performance of glass-fiber-reinforced polyester composites [42,45,46]. Additional investigations confirmed similar behavior for different fiber fractions and loading conditions [47–49]. One limitation of incorporating glass fiber into thermoset systems like unsaturated polyester is the weak compatibility between the polymer matrix and the reinforcing phase. As a result, additional surface treatments or bonding promoters are typically required to improve the interaction at their interface. Glass fibers have been extensively utilized as reinforcement, resulting in composites that demonstrate excellent mechanical, physical, and thermal performance across various fiber fractions [14–18]. In addition, chemical treatments of natural fibers using sodium hydroxide and acetic acid, improving the properties of the composite based on thermosetting resins, have been found in several studies [50–54].

In recent years, increasing awareness of ecological issues has sparked a resurgence in exploring fibers derived from natural, sustainable plant sources. A detailed understanding of fiber morphology, including cell size, shape, and chemical composition, is essential for accurately predicting their behavior in composite materials. In view of these factors, the present study focuses on Luffa cylindrica as a reinforcement. This fiber

is naturally abundant and offers multiple advantages, including renewability, biodegradability, a distinctive three-dimensional network structure, high strength, and a favorable initial modulus [55,56]. Composites reinforced with natural fibers are generally produced using conventional manufacturing techniques. Owing to these benefits, the automotive industry, for instance, has shown strong interest in incorporating such bio-based materials into different vehicle components [56].

The poor interfacial adhesion in natural fiber composites originates from the intrinsic chemical and physical dissimilarities between the fiber and the matrix. LF contains approximately 60 to 70% cellulose, 10 to 20% hemicellulose, 10 to 15% lignin, and a non-negligible fraction of waxes and pectins. The abundance of hydroxyl groups in cellulose and hemicellulose renders the fiber highly hydrophilic, whereas unsaturated polyester is hydrophobic. This polarity mismatch impedes proper wetting and leads to void formation at the interface. Furthermore, waxy substances on the fiber surface act as a physical barrier to mechanical interlocking, and the amorphous hemicellulose contributes to moisture uptake and dimensional instability [57,58].

Based on these considerations, it can be hypothesized that modifying the surface chemistry of LF through combined alkaline and acid treatments may improve their compatibility with unsaturated polyester matrices. In particular, alkaline treatment is expected to remove non-cellulosic amorphous components and expose reactive hydroxyl groups, while subsequent acetic acid treatment may induce partial esterification of these groups, thereby reducing fiber polarity and moisture affinity. This dual modification approach is anticipated to enhance fiber–matrix interfacial adhesion, promote more efficient stress transfer, and limit water diffusion pathways within the composite structure. Such a strategy could provide a synergistic improvement in both mechanical performance and hygrothermal stability compared to conventional single-step treatments.

The present study aims to investigate an original bio-composite system based on an unsaturated polyester resin (UPR) reinforced with Luffa cylindrica fibers (LF). While alkali treatment of LF has been widely reported, the originality of this work lies in the application of a combined NaOH–acetic acid surface modification designed to tailor the fiber surface chemistry through partial esterification of hydroxyl groups. This chemical strategy is intended to (i) reduce the intrinsic hydrophilicity of LF, (ii) enhance fiber–matrix interfacial compatibility, and (iii) promote more efficient stress transfer within the composite structure. Consequently, improved mechanical performance and reduced moisture sensitivity are expected. The developed composites are systematically evaluated in terms of tensile strength, impact resistance, hardness, density, and water absorption in order to establish a clear relationship between surface chemical modification, interfacial microstructure, and the resulting physico-mechanical behavior of UPR/LF composites.

2 Materials and Methods

2.1 Unsaturated Polyester Resin (UPR)

The unsaturated polyester resin was formulated using a prepolymer (density: 1.2 g/cm^3) obtained from LORN Chemicals. To initiate curing, 1.5 wt.% methyl ethyl ketone peroxide (MEKP) was incorporated into the system. The key characteristics of both the resin and the initiator are summarized in Table 1.

2.2 Luffa Fiber (LF)

The LF is an edible fibrous plant, with its interior composed of strong fibers interwoven into a dense network. Soft, flexible, hydrophilic, and durable, LF is recognized for its exceptional absorbent properties. Tables 2 and 3 provide details about the material characteristics and constituent makeup of LF, covering its physical attributes and chemical structure, respectively.

Table 1: Typical properties of polyester resin and MEKP catalyst.

Characteristic	Polyester Resin	MEKP Catalyst
Apparency	A blue liquid	Transparent liquid
Specific gravity	1.13	1.1
Density	1.1	1.18
Viscosity (mPa·s)	1800–2500 (25°C)	24 (20°C)
Compressive strength (MPa)	80	
Tensile strength (MPa)	6.8	-
Elastic modulus (GPa)	2	-
Impact resistance (kJ/m^2)	1.1	-
Electrical conductivity (mS/cm)	3.7	-
Thermal conductivity (W/m·K)	0.28	-

Table 2: Physical properties of LF.

Properties	Value
Density (g/cm^3)	0.92 ± 0.10
Diameter (μm)	270 ± 20
Micro fibrillar angle (°)	12 ± 2

Table 3: Chemical properties of LF.

Chemical Constituents %	Value
Cellulose %	63.0 ± 2.5
Lignin %	11.69 ± 1.2
Hemicelluloses %	20.88 ± 1.4
Ashes %	0.4 ± 0.10

2.3 Fiber Preparation

Prior to surface treatment, the LF was first chopped into pieces approximately 3 mm in length. These segments were subsequently soaked in a 5% NaOH solution maintained at 60°C for a duration of 2 h, aiming to eliminate contaminants from the surface. Once the process was completed, the fibers were taken out and repeatedly rinsed with distilled water until any residual alkali was completely removed and the texture no longer felt slick. In the final step, the cleaned fibers were left to dry naturally under ambient conditions for a period of three days.

The chemical modification of LF involves both NaOH and NaOH/acetic acid treatments, which induce changes in fiber surface chemistry. The NaOH treatment leads to the removal of amorphous constituents such as hemicellulose, lignin, pectin, and waxes, resulting in increased surface roughness and exposure of reactive hydroxyl groups from cellulose. This process enhances mechanical interlocking and improves interfacial adhesion with the unsaturated polyester matrix. The subsequent acetic acid (CH_3COOH) treatment partially neutralizes residual alkali and may promote limited esterification reactions with accessible hydroxyl groups, thereby reducing the hydrophilic character of the fibers. These combined effects contribute to improved compatibility between the fiber and the polymer matrix, as reflected in the enhanced mechanical properties and reduced water absorption of the composites.

2.3.1 Sodium Hydroxide (NaOH) Surface Treatment

LFs were soaked in an aqueous sodium hydroxide solution with a concentration of 5% by weight for a duration of one hour under ambient conditions. Then, the LFs were thoroughly rinsed with distilled

water containing a few drops of acetic acid to neutralize any remaining alkali. Subsequently, the LFs were washed under a continuous flow of distilled water to ensure complete removal of sodium hydroxide and to eliminate any soapy residue on the LF surface. After undergoing sodium hydroxide treatment, the LFs were initially left to dry in ambient conditions for a full day, followed by additional drying in an oven maintained at 80°C for twelve hours.

2.3.2 Combined Process (NaOH + CH_3COOH)

The LFs were treated by soaking them for one hour at ambient conditions in a mixture composed of 10 wt.% sodium hydroxide and 20 wt.% acetic acid, with 1 mL of concentrated sulfuric acid introduced to accelerate the reaction. After the treatment, the fibers were rinsed repeatedly using distilled water to ensure that any remaining chemicals were fully eliminated from their surfaces. Subsequently, the samples were left to dry under normal atmospheric conditions for 24 h and then further dried in an oven maintained at 80°C for 12 h.

2.4 Preparation of UPR/LF Composites

The required amount of UPR was weighed to prepare composite plates with an average thickness of 5 mm using wooden molds. The UPR matrix was mixed in a container, after which LF, untreated or treated with NaOH or NaOH + CH_3COOH, were incorporated at concentrations of 5, 10, 15, and 20 wt.%. Finally, 1.5 wt.% MEKP was added to ensure proper curing of the composite matrix. The mixtures obtained were poured onto a Teflon sheet on which the wooden mold was placed. A uniform distribution of the mixture over the surface of the mold was achieved using a wooden roller to remove any trapped air bubbles formed during mixing. All three bio-composite laminates were first allowed to harden under ambient conditions for one full day. Afterwards, they were placed in an oven and maintained at 45°C for 17 h to ensure the polymer matrix was fully set.

3 Materials Characterization and Testing

3.1 Fourier Transform Infrared Spectroscopy (FTIR)

FTIR is used to identify interactions between the matrix and the incorporated LF. FTIR analysis was conducted on both untreated and surface-treated LF, treated with sodium hydroxide (NaOH) and a combination of sodium hydroxide and acetic acid (NaOH + CH_3COOH). FTIR measurements were carried out using a Perkin Elmer instrument, scanning the spectral region between 4000 and 400 cm^{-1} at a resolution of 4 cm^{-1}.

3.2 Scanning Electron Microscopy (SEM)

To examine the interfacial structure between the reinforcement fibers and the surrounding matrix, the broken surfaces of the composite specimens were first covered with a fine gold film. This coating was applied using an automated sputter coating device (JEOL JFC-1600) to improve electrical conductivity during analysis. These surfaces were then examined using scanning electron microscopy (JEOL JSM 6390 LV). Additionally, the surface morphologies of the LF both before and after chemical treatments along with the corresponding composites, were observed with the same microscope.

3.3 Mechanical Tests

All mechanical tests were performed under controlled conditions following the corresponding ASTM standards. For each fiber content and surface treatment, multiple specimens were tested in order to ensure

the reliability of the results. All mechanical property values reported represent the average of five specimens, and the standard deviations are provided to indicate data reproducibility. This approach ensures statistical significance of the experimental data and allows proper evaluation of the variability associated with material preparation and testing procedures.

3.3.1 Tensile Tests

- The tensile test was performed on rectangular specimens with dimensions of 120 × 15 × 5 mm^3 to evaluate the tensile properties of the samples. Five specimens were tested for each fiber content, and the average values were reported. The tests were conducted using a GOTECH universal testing machine (UTM) equipped with a DT-W-20 kN dynamometer, at a crosshead speed of 3 mm/min and an initial gauge length of L_0 = 50 mm, in accordance with ASTM D3039 [59]. The tensile properties, including tensile strength (σ_r), strain at break (ε_r), and Young's modulus, were determined from the obtained stress–strain curves.

3.3.2 Impact Resistance Measurement

- The impact resistance of composites was tested using a Charpy/Izod impact machine per ASTM D256 [60]. Specimens measuring 65 × 15 × 5 mm^3 were subjected to an impact velocity of 1 m/s, using a 7.5 kg hammer dropped from 203.7 mm, delivering 1.4 J of energy. Specimens were supported as vertical cantilever beams and fractured by a single pendulum swing. Measurements were recorded at room temperature, with three tests per sample and average values reported.

3.3.3 Hardness Tests

- Shore D hardness measurements were performed in accordance with ASTM D2240-15 [61]. The test was conducted using a digital Shore D durometer (Model HD3000) equipped with a hardened steel conical indenter with a 30° included angle and a 0.1 mm radius spherical tip. A force of 44.5 N was applied. Ten measurements were taken on each composite sample at different locations, and the average value was reported to minimize the influence of surface heterogeneity inherent to natural fiber composites. All tests were carried out at 23 ± 2°C and 50 ± 5% relative humidity after conditioning the specimens for 48 h.

3.4 Physical Tests

3.4.1 Density

- Density evaluation was performed on three composite specimens following the ISO 1183-1 guideline [62]. The specimens were prepared by sectioning the molded, cured material with a diamond cutting tool assisted by a water stream. Each specimen had dimensions of 115 × 20 × 4 mm^3. The density (d) is determined using Eq. (1):

$$d = \frac{Wa \times \rho(fl)}{Wa - Wfl} + 0.0012 g/cm^3 \quad (1)$$

where $\rho(fl)$ is the density of the immersion liquid (g/cm^3); W_a and W_{fl} are the mass of the sample weighted in air (g) and in fluid, respectively; and 0.0012 corresponds to the density of air under normal conditions.

3.4.2 Water Absorption Test

- Water absorption tests followed ASTM D5229 standards [63]. Before testing, we recorded the initial weight of each sample. We immersed three samples of each composite in distilled water at room temperature. Every 24 h, we took the samples out, dried the surfaces with absorbent paper, and weighed them. After each measurement, we placed the samples back in the water. This process continued for several days until the weight of the samples remained constant. We calculated the water absorption percentage (WA, %) using Eq. (2) as follows,

$$WA(\%) = \frac{\text{Wet composite Weight (t)} - \text{Dry composite weight}}{\text{Dry composite weight}} \times 100\% \quad (2)$$

4 Results and Discussions

4.1 FTIR

Fig. 1 presents the FTIR spectra of untreated luffa fibers (LF) and fibers treated with NaOH and combined NaOH + CH_3COOH. The spectra exhibit characteristic absorption bands associated with the lignocellulosic structure of LF. The broad band observed around 3330–3350 cm^{-1} is assigned to O–H stretching vibrations arising from hydroxyl groups present in cellulose, hemicellulose, and lignin [52]. The bands located between 1030 and 1070 cm^{-1} correspond to C–O–C stretching vibrations and skeletal vibrations of cellulose polysaccharides [64]. The peak observed near 1428 cm^{-1} is attributed to CH_2 bending vibrations of cellulose, while the absorption bands around 1335–1360 cm^{-1} are associated with C–H and O–H bending vibrations of cellulose [52]. In addition, modifications in the FTIR spectra are observed after chemical treatment. The band around 1730–1740 cm^{-1}, generally attributed to the C=O stretching vibration of acetyl and uronic ester groups present in hemicellulose, becomes less pronounced after NaOH treatment, indicating partial removal of hemicellulosic constituents [65,66]. Moreover, the reduction in the intensity of bands associated with lignin-related structures suggests the elimination of non-cellulosic components from the fiber surface. These observations are consistent with the alkaline removal of amorphous constituents, including hemicellulose, lignin, waxes, and surface impurities.

Furthermore, fibers treated using the combined NaOH + CH_3COOH process exhibit a more distinct absorption band around 1735–1745 cm^{-1} together with a shoulder near 1240–1250 cm^{-1}. According to Maya et al. [65] and Mahima et al. [66], these bands can be attributed to carbonyl (C=O) stretching and C–O stretching vibrations associated with ester groups. Their appearance suggests that acetic acid treatment may induce partial hydroxyl groups on the fiber surface. This chemical modification contributes to reducing the hydrophilic character of the fibers and may improve their compatibility with the polyester matrix.

The FTIR spectra of neat UPR and UPR/LF composites are shown in Fig. 2. The broad absorption observed around 3543 cm^{-1} is associated with O–H stretching vibrations. Aromatic C–H stretching vibrations appear in the range 3075–3030 cm^{-1}, whereas aliphatic C–H stretching bands are detected around 2956 cm^{-1}. The strong absorption band located near 1730 cm^{-1} corresponds to the ester carbonyl (C=O) groups characteristic of the polyester matrix. In addition, bands between 1600 and 1400 cm^{-1} are assigned to C=C stretching vibrations, while the absorption band around 1266 cm^{-1} is related to C–O–C stretching vibrations of the polyester backbone [37].

The FTIR spectra of the UPR/LF composites exhibit characteristic absorption bands originating from both the polyester matrix and the lignocellulosic reinforcement. The presence of bands between 1040 and 1080 cm^{-1} confirms the contribution of cellulose through C–O–C stretching vibrations, while the absorption band around 1430 cm^{-1} is associated with CH_2 bending vibrations of cellulose [52]. Com-

pared with composites reinforced with untreated LF, those containing chemically treated fibers show less pronounced contributions from hydroxyl-rich components and a more evident presence of ester-related bands. These spectral changes support the effectiveness of the chemical treatments in modifying the fiber surface chemistry and improving the compatibility between the fibers and the polyester matrix [65,66]. The FTIR results are consistent with the proposed mechanisms of fiber modification, namely the partial removal of hemicellulose and lignin fractions during alkaline treatment and the possible formation of ester functionalities following the combined NaOH + CH_3COOH treatment. Such chemical modifications reduce the hydrophilic nature of the fibers and are expected to enhance fiber–matrix interfacial adhesion, which is in agreement with the improved mechanical performance and fracture morphology observed in the SEM analysis [65–67].

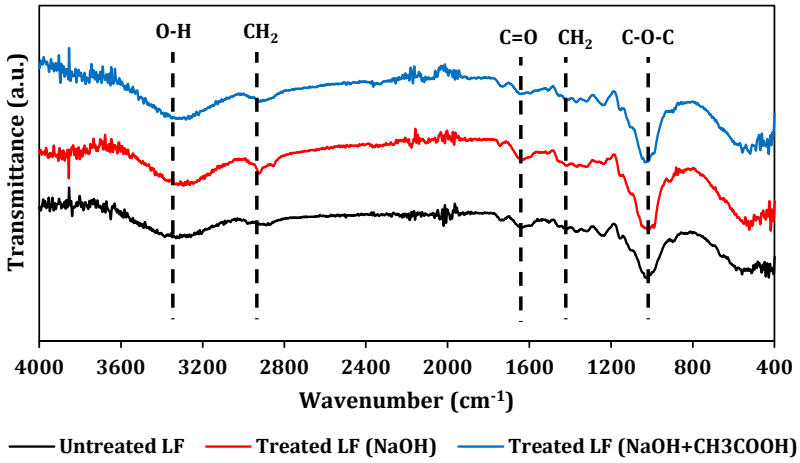

Figure 1: FTIR spectra of untreated LF, treated with (NaOH) and (NaOH + CH_3COOH).

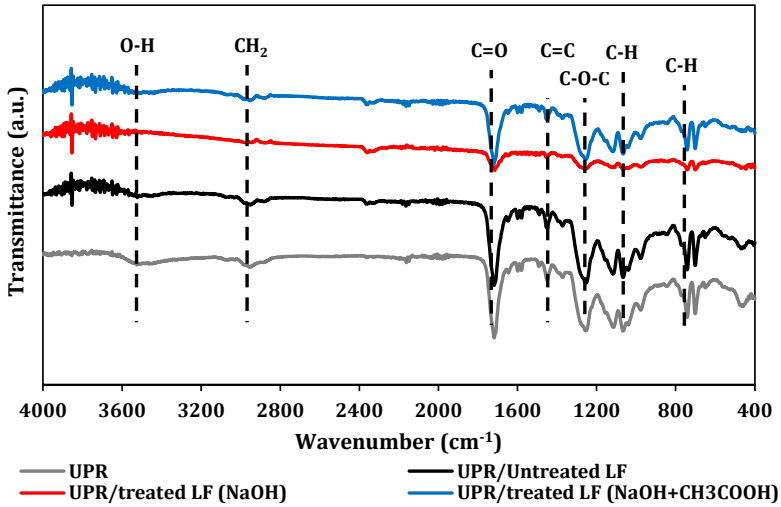

Figure 2: FTIR spectra of UPR, untreated UPR/LF composite, UPR/LF treated with (NaOH), and UPR/LF treated with (NaOH + CH_3COOH).

4.2 Mechanical Properties of Composites UPR/LF

4.2.1 Tensile Properties

The variations in the tensile properties, particularly tensile strength, strain at break, and Young's modulus of the UPR/LF composites as a function of fiber content and surface treatment, are presented in Fig. 3, Fig. 4, and Fig. 5, respectively. According to Fig. 3, which illustrates the evolution of tensile strength with LF content, an increase is observed compared with the neat UPR matrix up to a fiber loading of 10 wt.%, followed by a decrease at higher loadings. This improvement becomes more pronounced when the fibers are chemically treated with NaOH or with the combined NaOH + CH_3COOH process. However, increasing the fiber content beyond the optimal level promotes fiber agglomeration, which disrupts the structural continuity of the composite and generates stress concentration zones that may initiate brittle failure. The enhancement in tensile strength is mainly attributed to the reinforcing and stiffening effect of the incorporated fibers.

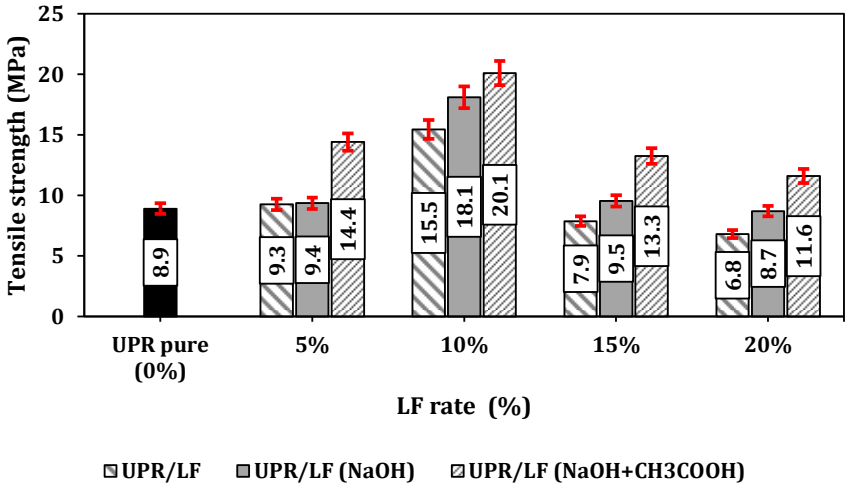

Figure 3: Variations in the tensile strength of UPR/LF composites as a function of the fiber content and surface treatment by (NaOH) and (NaOH + CH_3COOH).

Chemical treatment modifies the surface chemistry of luffa fibers and improves their compatibility with the unsaturated polyester matrix through several complementary mechanisms. During alkaline treatment, some cellulose hydroxyl groups are converted into more reactive alkoxide species (–O–Na^+), which may participate in transesterification reactions with the ester functionalities of the UPR during curing. In addition, residual hydroxyl groups remaining on the treated fiber surface can establish hydrogen-bonding interactions with the carbonyl groups of the polyester matrix. Simultaneously, the removal of hemicellulose, lignin, and surface impurities increases the surface roughness of the fibers, thereby promoting stronger mechanical interlocking between the reinforcement and the matrix.

These interfacial modifications are clearly reflected in the mechanical performance of the composites. At the optimal fiber loading of 10 wt.%, the tensile strength increased from 15.5 ± 1.8 MPa for untreated LF composites to 18.1 ± 1.9 MPa and 20.1 ± 2.1 MPa for NaOH-treated and NaOH + CH_3COOH-treated LF composites, respectively. Compared with the neat UPR matrix, this corresponds to an increase of approximately 126% for the combined treatment. Similarly, both the strain at break and Young's modulus increased after chemical treatment, confirming the improvement in stress transfer efficiency between the fibers and the polyester matrix. SEM observations further support these findings by revealing reduced

fiber pull-out and improved matrix adhesion around treated fibers compared with untreated composites. Therefore, the enhanced interfacial adhesion can be attributed to the combined contribution of possible covalent interactions through transesterification, hydrogen bonding, and improved mechanical anchoring at the fiber–matrix interface [68,69]. The superior performance obtained with the combined NaOH + CH_3COOH treatment also demonstrates that reducing the hydrophilic character of LF improves fiber–matrix compatibility, thereby enhancing the overall mechanical performance of the developed bio-composites.

Fig. 4 shows the evolution of strain at break for the different composites. The strain at break increased from 4.64% for neat UPR to 6.2%, 7.35%, and 8.85% for UPR/LF composites reinforced with untreated LF, NaOH-treated LF, and NaOH + CH_3COOH-treated LF, respectively, at a fiber loading of 10 wt.%. Overall, the tensile behavior of the composites was improved after chemical treatment, particularly for the combined NaOH + CH_3COOH process. This enhancement is attributed to improved fiber dispersion within the matrix and stronger interfacial adhesion resulting from the chemical modification of the fiber surface [67]. Beyond 10 wt.% fiber content, the strain at break decreases for all composites. This reduction may be related to fiber agglomeration, insufficient matrix wetting, and reduced matrix continuity at high fiber loadings. In addition, homogeneous fiber dispersion within the matrix is a key factor governing efficient stress distribution and improved ductility. Conversely, at higher fiber loadings, inadequate fiber dispersion, fiber agglomeration, and incomplete matrix impregnation may generate stress concentration sites, leading to a reduction in tensile strength and elongation at break. Similar behavior has been reported for sisal fiber and luffa fiber-reinforced polymer composites, where excessive fiber content compromises fiber distribution and interfacial bonding, thereby deteriorating the mechanical performance [70,71].

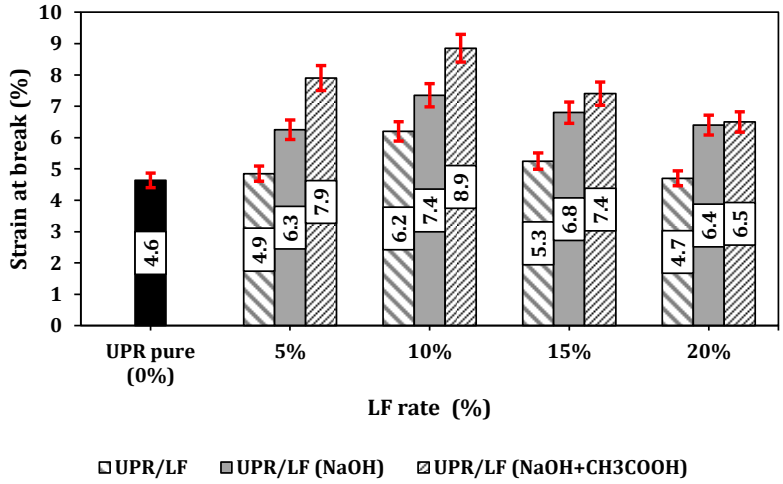

Figure 4: Variations in the strain at break of UPR/LF composites as a function of the fiber rate and surface treatment by (NaOH) and (NaOH + CH_3COOH).

The tensile modulus (Young's modulus) of the UPR/LF composites was determined from the initial linear region of the stress–strain curves and is presented in Fig. 5. The results indicate that the modulus increases with fiber loading up to 10 wt.% for treated fibers, reflecting enhanced composite stiffness and more efficient stress transfer between the reinforcement and the matrix. This improvement is particularly pronounced for composites reinforced with LF treated by the combined NaOH + CH_3COOH process, confirming the beneficial effect of chemical treatment on interfacial adhesion. The increase in modulus is also associated with the removal of amorphous constituents and the improved fiber–matrix interaction resulting from surface modification. However, at higher fiber contents, a slight decrease in modulus is

observed due to fiber agglomeration, insufficient resin impregnation, and reduced matrix continuity. These results are consistent with the tensile strength behavior and further confirm the critical role of interfacial quality in controlling the mechanical performance of the developed composites.

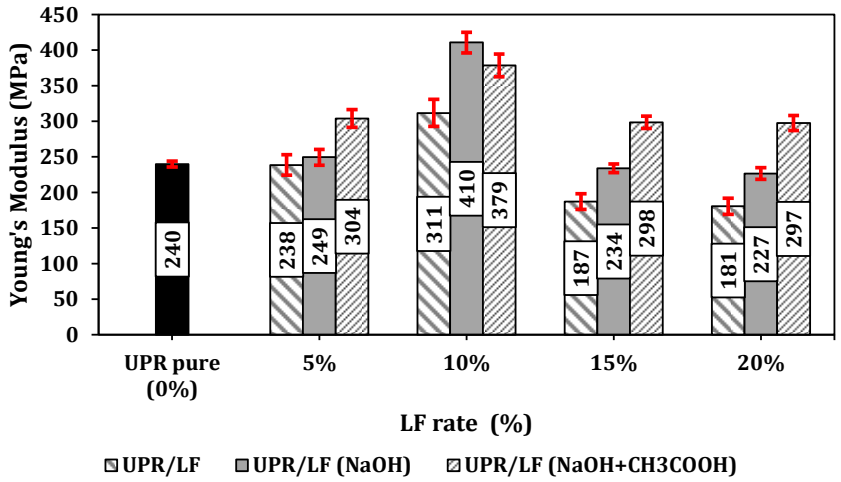

Figure 5: Young's Modulus of UPR/LF composites as a function of the fiber content and surface treatment by (NaOH) and (NaOH + CH_3COOH).

4.2.2 Resilience of UPR/LF Composites

- The impact resistance without notching of the UPR/LF composites as a function of the fiber content and the surface treatment is represented by Fig. 6. The curves clearly show that the resilience of bio-composites increases with fiber content up to 10–15%, then decreases. We can also discern the effect of treating the surface of the fiber. Thus, bio-composites with surface treatment have the highest impact resistance. Furthermore, reinforcement/matrix adhesion is improved thanks to the surface treatment, which makes it possible to promote, for a certain percentage, contact at the interface between the two components of the material [41].
- The increase in resilience of the whole bio-composites reinforced with LF treated with NaOH and with (NaOH + CH_3COOH) relative to the UPR matrix may be due to the chemical treatment to eliminate waxy impurities, lignin, and hydroxyl groups on the surface of the LF [72]. From LF content of 15%, the opposite occurs because the effects of phenomena at the interface (formation of aggregates and lack of adhesion) dominate because of the high concentration of the natural LF and the low contribution of resin likely to diffuse into the fiber (there is not enough remaining when the reinforcement rate reaches 20%). The lack of good wettability of the luffa fibers by the UPR matrix leads to problems, resulting in a decrease in mechanical properties [73].

4.2.3 Shore Hardness of UPR/LF Composites

The variations in hardness as a function of the fiber content and the surface treatment are shown in Fig. 7. An increase is noted for the bio-composites reinforced with 5 and 10% of LF. This increase is due to the longer than the LF is treated by (NaOH) and (NaOH + CH_3COOH). The treatment strengthens the interface between the LF and the UPR [74]. In addition, voids and hydroxyl groups were removed from the surface due to surface treatment. The chemical modification caused a structural change to the surface of the LF, which roughened the surface and consequently increased the hardness of the composite. Also, a reduction in hardness is observed at the highest rates, namely 15 and 20%.

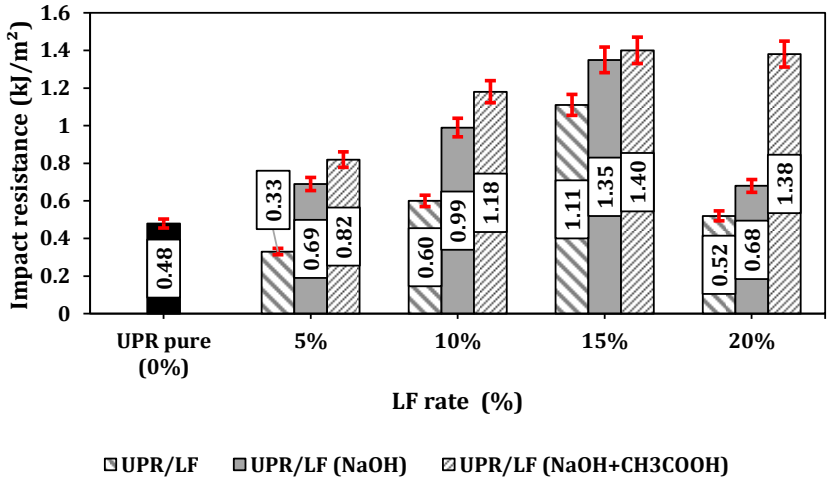

Figure 6: Impact resistance of UPR/LF composites as a function of the fiber content and surface treatment by (NaOH) and (NaOH + CH_3COOH).

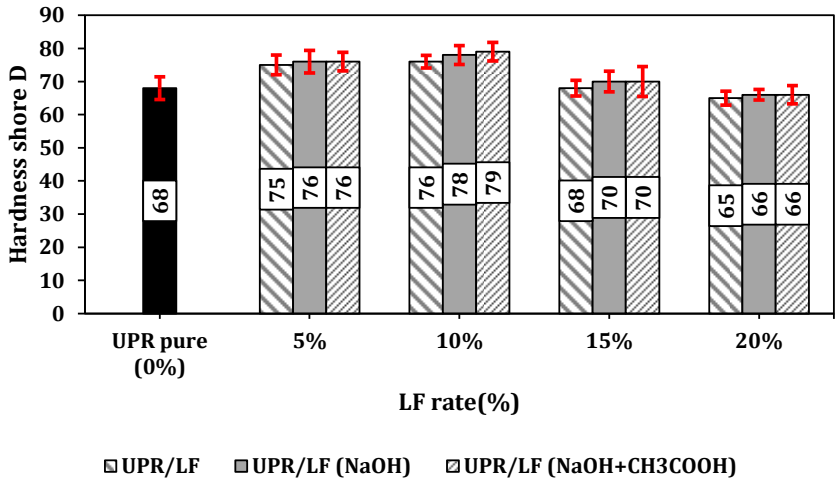

Figure 7: Variations in the Shore hardness D of UPR/LF composites as a function of the fiber content and surface treatment with (NaOH) and (NaOH + CH_3COOH).

4.2.4 Density of UPR/LF Composites

The density of the UPR/LF composites as a function of the fiber rate and surface treatment are reported in Fig. 8. The low density of the LF led to variations in the density of the resin 1.2. Thus, by increasing the fiber rate of 5, 10, 15, and 20%, the density of the bio-composites reinforced with untreated LF was 1.18, 1.17, 1.16, and 1.13, respectively. In addition, the more the LF is treated with (NaOH + CH_3COOH), the more the density decreases. This represents an additional advantage for the UPR/LF composite, since lightweight characteristics are highly desirable in structural applications while maintaining adequate mechanical performance. Therefore, the incorporation of chemically treated luffa fibers contributes to the development of lightweight bio-composites with improved mechanical properties, mainly due to enhanced fiber–matrix interfacial adhesion and more efficient stress transfer between the reinforcement and the polymer matrix [74].

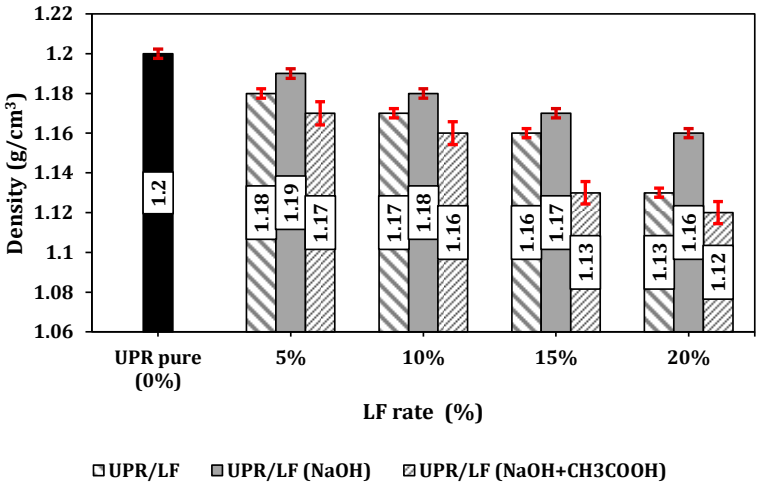

Figure 8: Variations in the density of UPR/LF composites as a function of the fiber rate and surface treatment by (NaOH) and (NaOH + CH_3COOH).

4.2.5 Influence of the LF Rate and Surface Treatment on the Water Absorption of UPR/LF Composites

Fig. 9 presents the moisture uptake data. All examined composites exhibit a comparable trend in their absorption patterns. A rapid intake of water occurs during the early period (0–48 h), after which the materials begin to approach saturation [75,76]. For composites reinforced with modified luffa fibers, a steady state is achieved around 48 h. In contrast, composites containing unmodified fibers continue to take in small amounts of water beyond this period. The absorption rate was lower for UPR/treated LF than for UPR/untreated LF after 250 h of exposure to water. UPR/untreated LF composites exhibit higher water absorption rates due to the hydrophilic nature of cellulose. The high-water absorption leads to changes in the dimensional properties of the samples. UPR/Untreated LF composites showed the highest water absorption of all composites. Moisture uptake is notably reduced when the fibers are chemically modified with sodium hydroxide (NaOH), and this reduction becomes even more significant when a combined sodium hydroxide and acetic acid treatment is applied, in comparison to untreated fibers. This improvement is mainly linked to stronger bonding at the interface between the reinforcement and the polymer matrix, as well as an increase in the fibers' resistance to water. The modification of hydroxyl functionalities in the fiber structure plays a key role in limiting water penetration, thereby enhancing the overall compatibility between the fibers and the matrix. Thus, (NaOH) treatment of LF reduced the polar groups in the fiber by replacing some of the hydroxyl groups on the surface of the fibers.

It is important to note that the initial moisture content of LF prior to composite fabrication was not directly measured in this study. However, the influence of chemical treatments on the hydrophilic behavior of the fibers can be indirectly assessed through the water absorption response of the resulting composites. The obtained results clearly demonstrate that all composites exhibit an initial rapid water uptake, followed by a gradual approach toward saturation. In the case of composites reinforced with chemically treated fibers, a stabilization of water absorption is reached earlier compared to those containing untreated fibers, which continue to absorb water over a longer period. This behavior indicates that alkaline (NaOH) and combined NaOH/acetic acid treatments effectively reduce the hydrophilicity of the fibers and improve interfacial compatibility with the polyester matrix. The reduction in water uptake is attributed to the partial removal or modification of hydroxyl-rich components (such as hemicellulose and surface impurities), which limits the availability of polar sites for water interaction. In addition, improved fiber–matrix adhesion

reduces interfacial voids and restricts water diffusion pathways, thereby enhancing the overall moisture resistance of the composites.

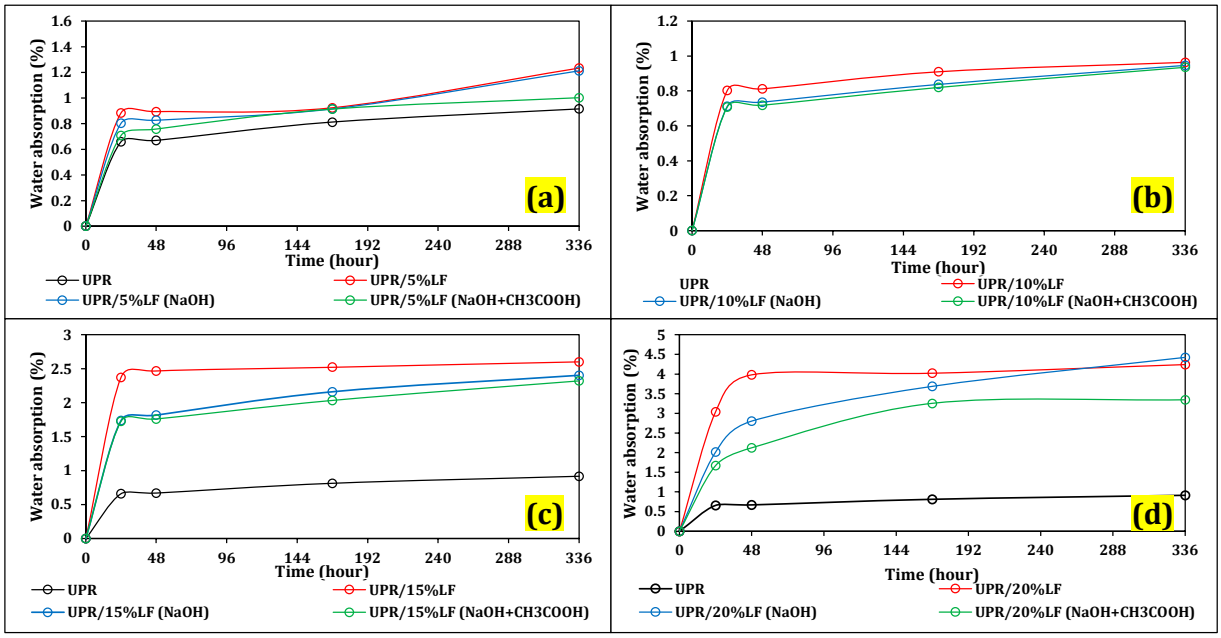

Figure 9: Influence of fiber rate and surface treatment on water absorption of UPR, 5% LF/UPR (**a**), 10% LF/UPR (**b**), 15% LF/UPR (**c**) and 20% LF/UPR (**d**).

4.2.6 Morphology of UPR/LF Composites

Fig. 10 shows the SEM images of untreated LF and LF treated with (NaOH) and (NaOH + CH_3COOH), respectively. The LF shape appears to be a long strip with a non-planar surface and fiber diameters ranging from 12 to 30 μm. Fig. 10a (untreated LF) shows the presence of a thin layer of lignin covering the cellulose fibrils. These results, compared with those shown in Fig. 10b (LF treated with NaOH), indicate that alkali treatment removes waxy substances present on the surface of untreated LF. Certain modification methods applied to LFs can enhance their ordered internal arrangement by eliminating non-crystalline constituents like lignin and hemicellulose. As illustrated in Fig. 9c, fibers subjected to the dual treatment (NaOH followed by CH_3COOH) exhibit noticeable surface abrasions, likely due to the stripping away of outer protective layers. This combined approach appears to deliver superior results, as the resulting surface texture becomes more favorable for bonding with the polyester phase, thereby improving reinforcement performance in composite fabrication processes.

In addition to surface observations, the internal structure of LF is characterized by a highly porous shape composed of interconnected lumens and cell walls arranged in a radial pattern. Although the present SEM analysis mainly focuses on surface morphology and fiber–matrix interfacial features, it is important to note that this hierarchical structure plays a key role in the mechanical behavior and fluid transport properties of the fibers. The presence of lumens contributes to low density and energy absorption capacity, while the multilayered cell wall structure governs stiffness and strength. Cross-sectional SEM analysis of Luffa fibers reveals a highly porous structure composed of vascular bundles and parenchyma cells. After alkaline and acetic acid treatments, a noticeable reduction in lumen diameter and removal of non-cellulosic constituents from the cell walls were observed, leading to fiber densification. This structural change enhances the fiber's load-bearing capacity and improves interfacial contact with the polyester matrix. A

detailed investigation of the radial cross-section, requiring specific sample preparation techniques, will be addressed in future work to better correlate internal morphology with composite performance.

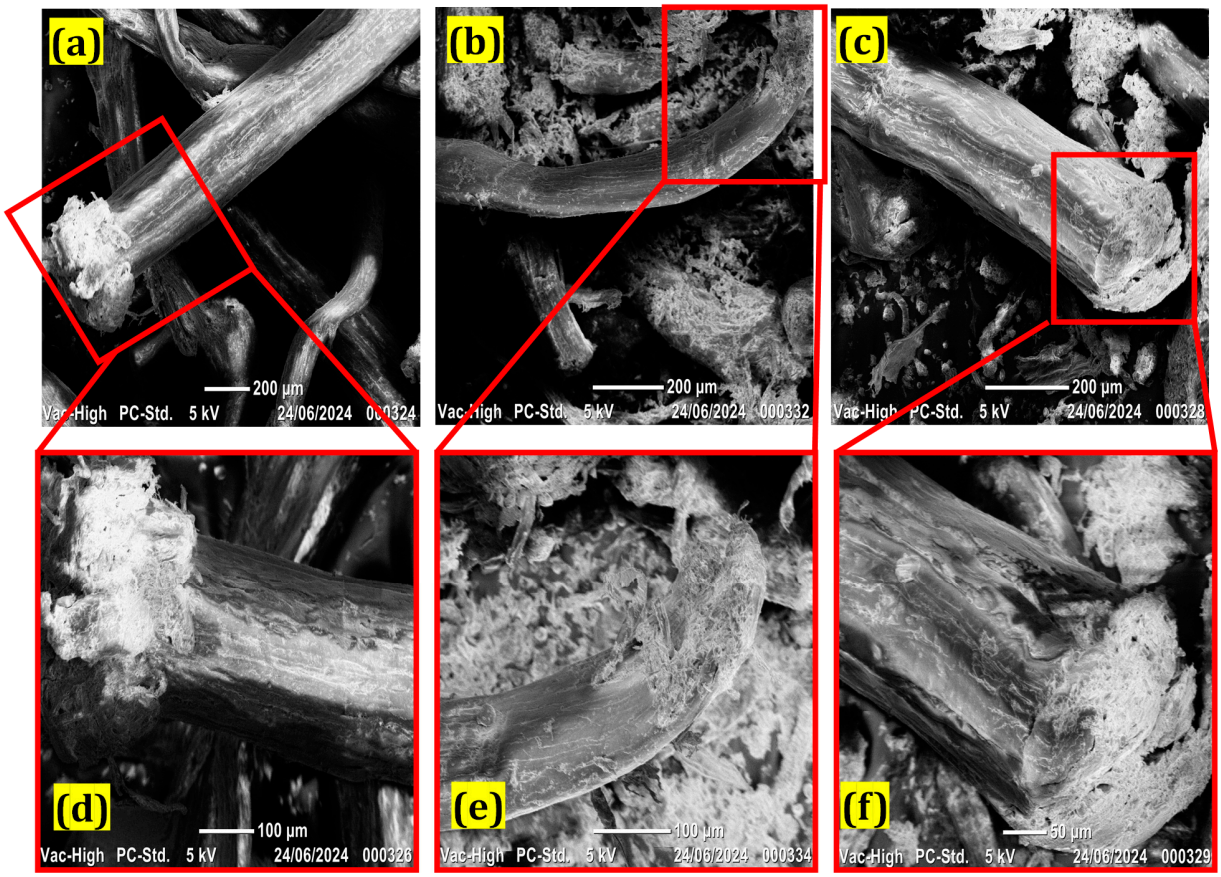

Figure 10: SEM images of untreated LF (**a**), LF treated with NaOH (**b**), and LF treated with the combined process NaOH + CH_3COOH (**c**), along with their corresponding higher-magnification micrographs (**d**–**f**), highlighting surface morphology details after each treatment.

Fig. 11 presents SEM micrographs of the fractured surfaces after impact testing. Clear variations can be seen in how the fibers interact with the polymer matrix when comparing untreated and chemically modified LF composites. As illustrated in Fig. 11a, the composite containing untreated fibers exhibits a weak fiber-matrix interface, indicating insufficient bonding and a lack of effective interaction between the reinforcement and the unsaturated polyester resin. The untreated LF was easily pulled out from the UPR matrix which indicates weak interfacial bonding and consequently inefficient load transfer between reinforcement and polymer. In contrast, the composites containing chemically treated LF (Fig. 11b–d) show that fractured fiber remnants remain firmly trapped within the matrix after failure, demonstrating improved interfacial compatibility between the fibers and the UPR. This behavior suggests that the fibers were able to carry and sustain the stress transferred from the surrounding matrix, reflecting enhanced stress-sharing efficiency. Such performance is associated with a well-developed interface that promotes effective load distribution across the composite structure, which is essential for strengthening the material system [77]. Furthermore, noticeable fiber deformation along with the uneven and rugged nature of the fractured surfaces, especially in samples reinforced with 15% and 20% fiber content, which provides additional confirmation of strong interfacial bonding. The presence of hydroxyl functionalities on the

treated fiber surfaces is also likely to promote stronger intermolecular attraction, particularly through hydrogen bonding with the polyester matrix, thereby further improving adhesion.

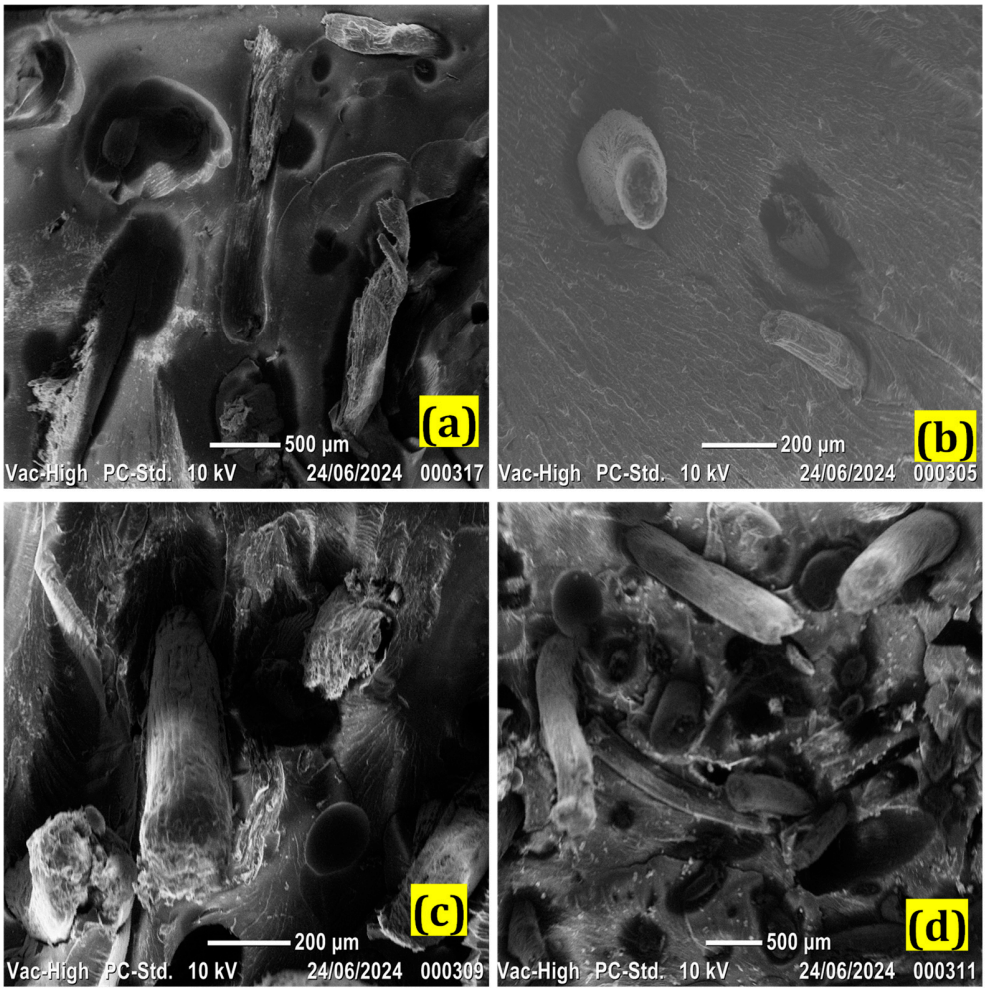

Figure 11: SEM images of UPR composites reinforced with (**a**) 10% untreated LF, (**b**) 5% LF treated with (NaOH + CH_3COOH), (**c**) 15% treated LF with (NaOH + CH_3COOH), and (**d**) 20% LF treated with (NaOH + CH_3COOH).

4.3 Statistical Analysis

4.3.1 Design of Experiments Using Statistical Response Surface Method

Design-Expert® software (Version 13) was utilized to perform a structured statistical analysis based on a full factorial experimental design [78,79]. In accordance with the developed experimental matrix, a 3 × 4 general factorial design was adopted to systematically investigate the combined effects of fiber surface treatment type TT and LF replacement rate on the physical and mechanical properties of the developed polyester-based bio-composites. The experimental design was structured around two independent variables: the type of fiber treatment (Factor A) and the fiber replacement rate (Factor B). Factor A was investigated at three levels, namely untreated fibers (−1), NaOH-treated fibers (0), and fibers subjected to a combined NaOH/acetic acid treatment (+1), representing different chemical surface modification strategies aimed at improving fiber–matrix interfacial adhesion. Factor B corresponded to the fiber replacement rate and was examined at four levels: 5% (−1), 10% (0), 15% (+0.5), and 20% (+1), reflecting the progressive incorporation

of LF into the UPR matrix. The experimental design matrix adopted for the factorial analysis is presented in Table 4.

Table 4: Experimental design matrix and corresponding measured properties.

Mix ID	Type of Treatment (TT)	LF Remplacement Rate (%) (LF)
1	−1	−1
2	0	−1
3	+1	−1
4	−1	0
5	0	0
6	+1	0
7	−1	+0.5
8	0	+0.5
9	+1	+0.5
10	−1	+1
11	0	+1
12	+1	+1

The developed regression equations for the evaluated responses are given in Eqs. (3)–(8) below (coded form):

$$Tensile\ Strength = 5.8083 + 4.05 \times TT + 1.4257 \times LF - 0.074 \times TT \times LF \quad (3)$$

$$Strain\ at\ Break = 4.975 + 1.725 \times TT + 0.3917 \times LF - 0.042 \times TT \times LF \quad (4)$$

$$Impact\ Strength = -0.2625 + 0.175 \times TT + 0.2028 \times LF + 0.0077 \times TT \times LF \quad (5)$$

$$Shore\ Hardness = 74.5833 + 1 \times TT + 0.65 \times LF - 0.01 \times TT \times LF \quad (6)$$

$$Density = 1.2033 - 0.0050 \times TT - 0.00127 \times LF - 0.00020 \times TT \times LF \quad (7)$$

$$Water\ Absorption = 1.8192 + 0.135 \times TT - 0.2361 \times LF - 0.0257 \times TT \times LF \quad (8)$$

The two-dimensional contour plots derived from the developed factorial models (Fig. 12) illustrate the combined effects of LF surface treatment type (TT) and LF replacement rate on the physical and mechanical behavior of the LF/UPR composites. For tensile strength (MPa), an improvement is observed with increasing LF content up to an optimal level, particularly for chemically treated fibers. The transition from untreated to NaOH and NaOH/acetic acid treatments results in higher strength values, which can be attributed to enhanced interfacial adhesion and improved stress transfer between the LF and the UPR matrix. However, at higher fiber loadings, slight reductions may occur due to fiber agglomeration and dispersion issues. A similar trend is noted for strain at break (%), where both the increase in LF content and the application of chemical treatments contribute to improved ductility. The combined NaOH/acetic acid treatment exhibits the most pronounced effect, indicating better fiber-matrix compatibility and reduced interfacial defects. However, untreated fibers show lower deformation capacity due to weaker bonding. For impact strength (kJ/m^2), the contour plots reveal a significant enhancement with increasing fiber incorporation, especially for treated fibers. This behavior is associated with the energy absorption mechanisms provided by the fibers, such as pull-out and crack bridging, which are more effective when interfacial adhesion is improved through chemical modification. Regarding Shore hardness (D), a gradual increase is observed with fiber content,

with treated fibers contributing to slightly higher hardness values due to improved interfacial cohesion and matrix stiffening. The effect of treatment remains moderate compared to fiber loading, indicating that hardness is primarily governed by composite densification. In terms of density (g/cm^3), the contour diagrams indicate a slight decrease with increasing fiber replacement rate, reflecting the lower density of LF compared to the polyester matrix. Fiber treatment has a minimal influence on density, although a marginal reduction may be observed due to structural modifications at the fiber surface.

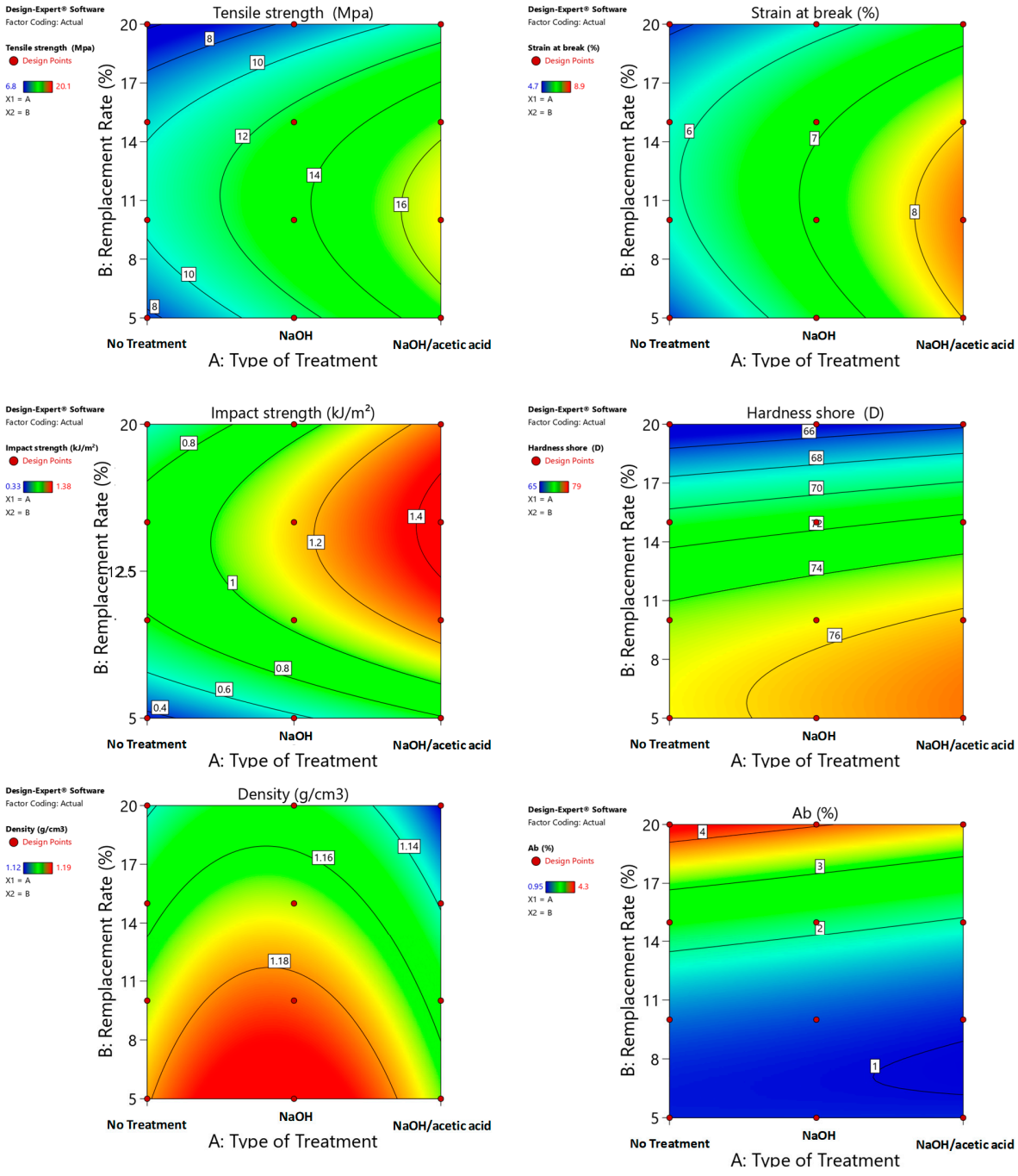

Figure 12: Surface response contours depicting the interaction of type of treatment (TT) and LF rate replacement on composite behavior.

Finally, water absorption (%) shows a decreasing trend with increasing fiber content, particularly for chemically treated fibers. The NaOH/acetic acid treatment significantly reduces water uptake by modifying the hydrophilic nature of the fibers and improving interfacial sealing, thereby limiting moisture penetration pathways within the composite. The contour plots clearly demonstrate that fiber surface treatment plays a crucial role in enhancing composite performance, while fiber replacement rate governs the balance between mechanical improvement and structural integrity. Combined chemical treatment emerges as the most effective approach, significantly improving interfacial bonding and mitigating the limitations associated with higher fiber contents.

4.3.2 Model Validation

The statistical adequacy of the developed regression models [74–76] was evaluated using the fit statistics presented in Table 5 and the ANOVA results summarized in Table 6. For all measured properties: tensile strength, elongation at break, impact resistance, Shore hardness, density, and water absorption, the coefficient of determination (R^2) remained very high, between 0.9047 and 0.9948. This shows that the proposed factorial models are able to account for over 90% of the observed variation in the experimental results. Furthermore, the close correspondence between adjusted R^2 and predicted R^2 values demonstrates that the models are stable and possess strong predictive reliability.

Table 5: Statistical validation and goodness-of-fit parameters of the developed model.

Response	Tensile Strength (MPa)	Strain at Break (%)	Impact Strength (kJ/m^2)	Hardness Shore D (%)	Density (g/cm^3)	Water Absorption (%)
Standard deviation	0.7396	0.3801	0.1482	0.5000	0.0075	0.2723
Mean	11.44	6.56	0.9258	72.08	1.16	2.12
R^2	0.9804	0.9483	0.9047	0.9948	0.9383	0.9754
Predicted R^2	0.9214	0.7933	0.6187	0.9791	0.7531	0.9016
Adjusted R^2	0.9640	0.9052	0.8252	0.9904	0.8868	0.9549
Adequate precision	24.9548	15.0082	11.4763	38.8909	13.9140	17.5307

Table 6: Analysis of variance (ANOVA) results.

Response	Tensile Strength (MPa)	Strain at Break (%)	Impact Strength (kJ/m^2)	Hardness Shore (D)	Density (g/cm^3)	Water Absorption (%)
Sum of squares	163.73	15.90	1.25	285.42	0.0051	17.64
D_f	5	5	5	5	5	5
Mean square	32.75	3.18	0.2501	57.08	0.0010	3.53
F-value	59.87	22.02	11.39	228.33	18.24	47.57
p-value	0.0001	0.0009	0.0051	0.0001	0.0014	0.0001
Remarks	Significant	Significant	Significant	Significant	Significant	Significant

The ANOVA results further demonstrate the statistical significance of the regression models. The F-values obtained for all responses are relatively high, while the corresponding *p*-values are lower than 0.05, indicating that the models are statistically significant at a 95% confidence level. These results confirm that the selected factors, namely the type of fiber treatment (Factor A) and the fiber replacement rate (Factor B), as well as their interaction, have a significant influence on the mechanical and physical properties of the developed composites.

The comparison between calculated and experimental results for all outputs (Fig. 13) indicates that the data points lie very near the diagonal 45° line. This close clustering reflects a high level of correspondence between observed measurements and model predictions. It also verifies that the developed factorial models are dependable and effectively capture the behavior of the composite system under study.

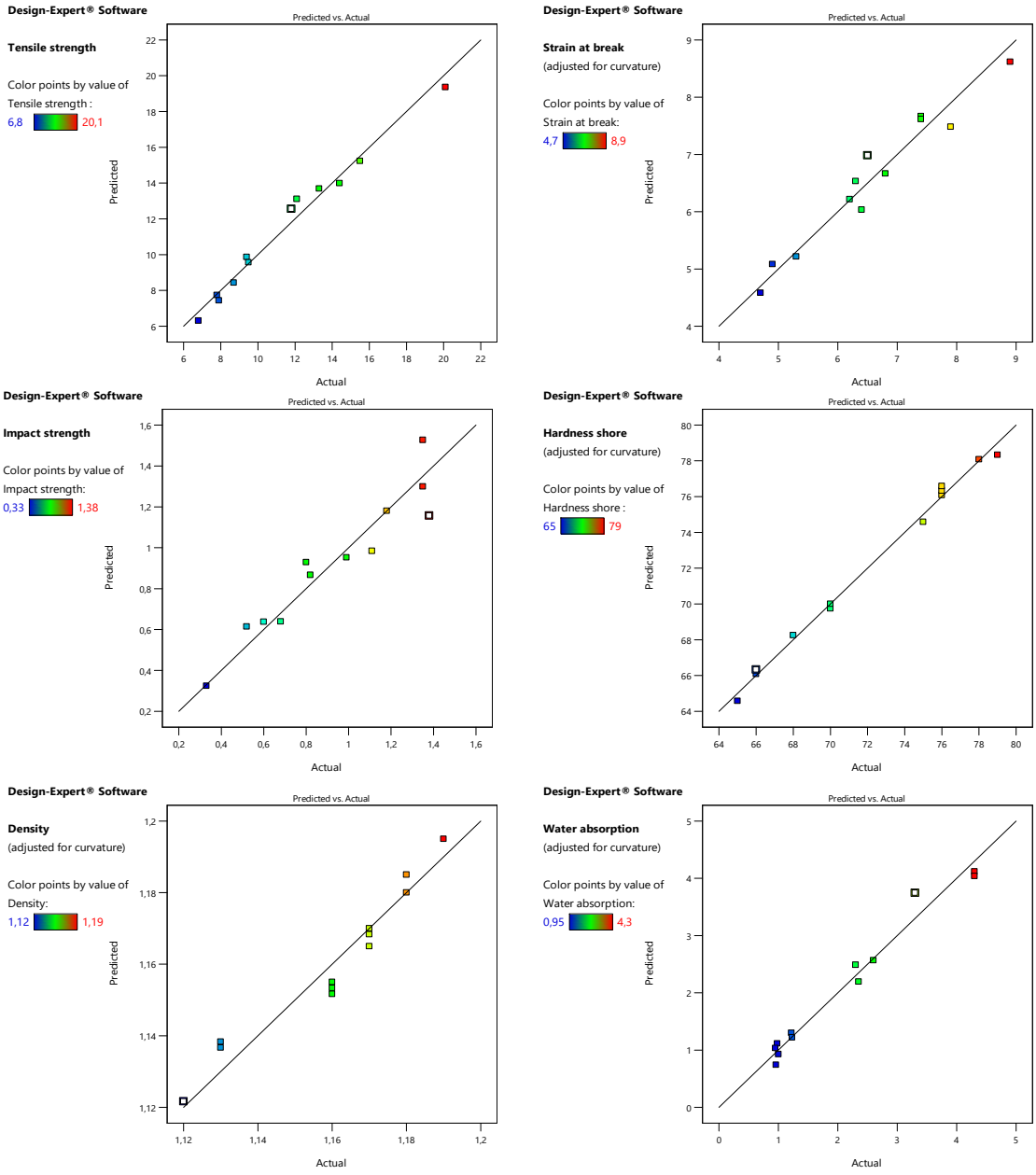

Figure 13: Correlation between actual and predicted response.

4.3.3 Factorial Optimization and Experimental Validation

It can be challenging to determine the optimal combination of input variables when multiple performance criteria must be simultaneously satisfied [80–82]. Therefore, a multi-objective optimization approach was carried out based on the developed factorial regression models to identify the most suitable

combination of fiber treatment type (TT) and fiber replacement rate (LF). The optimization aimed to achieve a compromise between the mechanical and physical responses of the developed composites.

The independent variables considered were fiber surface treatment (Factor A) and fiber replacement rate (Factor B), while the target responses included tensile strength, strain at break, impact strength, Shore hardness, density, and water absorption. The optimization criteria were defined that mechanical properties (tensile strength, strain, impact strength, and hardness) were maximized, whereas density and water absorption were minimized, as summarized in Table 7.

A desirability function approach was employed to evaluate the optimization performance, where the desirability value ranges from 0 to 1, with values closer to 1 indicating a more optimal solution. The optimization results revealed that the combined NaOH/acetic acid treatment and a fiber replacement rate of 10% represent the best compromise among all responses.

Under these optimal conditions, the predicted responses were tensile strength of 19.35 MPa, strain at break of 8.61%, impact strength of 1.18 kJ/m^2, Shore hardness of 78.33%, density of 1.155 g/cm^3, and water absorption of 0.741% (Table 8). The overall desirability of the solution was found to be 0.835 (83.5%), indicating a high level of optimization considering the multiple and sometimes conflicting objectives.

To validate the reliability of the developed factorial models and the optimization results, experimental tests were conducted using the optimal factor combination (Fig. 14). The experimental results showed strong agreement with the predicted values, with deviations of 3.73%, 3.26%, 0.00%, 0.84%, 0.43%, and 2.21% for tensile strength, strain at break, impact strength, hardness, density, and water absorption, respectively.

All experimental errors were found to be lower than 5%, confirming the high accuracy, robustness, and predictive capability of the developed models. This close agreement demonstrates that the factorial design methodology and the applied optimization strategy are reliable tools for predicting and optimizing the performance of polyester-based bio-composites reinforced with treated LF.

Table 7: Objective optimization criteria.

Variable/Response	Optimization Criteria/Goal	Lower Limits	Upper Limits
A: TT	is in range	No Treatment	NaOH/acetic acid
B: LF rate	is in range	5	20
Tensile strength (MPa)	maximize	6.8	20.1
Strain at break (%)	maximize	4.7	8.9
Impact strength (kJ/m^2)	maximize	0.33	1.38
Hardness shore D (%)	maximize	65	79
Density (g/cm^3)	minimize	1.12	1.19
Water absorption (%)	minimize	0.95	4.3

Results confirm that the combined chemical treatment enhances interfacial adhesion, leading to improved mechanical performance and reduced water absorption, while the optimal fiber content ensures a balance between reinforcement efficiency and structural integrity.

The observed optimum in mechanical performance at 10 wt.% fiber content can be explained by considering both microstructural dispersion and interfacial phenomena. At low fiber loadings, the fibers are well dispersed within the matrix, ensuring effective stress transfer through a sufficiently wetted interface. At approximately 10 wt.%, an optimal balance is achieved between fiber content and matrix continuity, allowing efficient load distribution and maximized interfacial interactions. This condition can be associated with a critical threshold related to interfacial coverage and the onset of fiber network interactions. At higher fiber contents, however, the increased likelihood of fiber agglomeration and fiber–fiber contacts

leads to poor matrix impregnation, the formation of voids, and stress concentration sites. These effects limit the efficiency of stress transfer and result in reduced mechanical performance. This behavior is consistent with classical composite theories involving percolation thresholds and interfacial saturation effects.

Table 8: Multi-objective optimization solution, optimum factors and desirability.

Variable/Response	Solution	Experimental Validation	Error (%)
A: TT	NaOH/acetic acid	-	-
B: LF rate	10%	-	-
Tensile strength (MPa)	19.35	20.1	3.73
Strain at break (%)	8.61	8.9	3.26
Impact strength (kJ/m^2)	1.18	1.18	0
Hardness shore (D)	78.33	79	0.84
Density (g/cm^3)	1.155	1.16	0.43
Water absorption (%)	0.741	0.96	2.218
Solution Desirability	0.835 (83.5%)	-	-

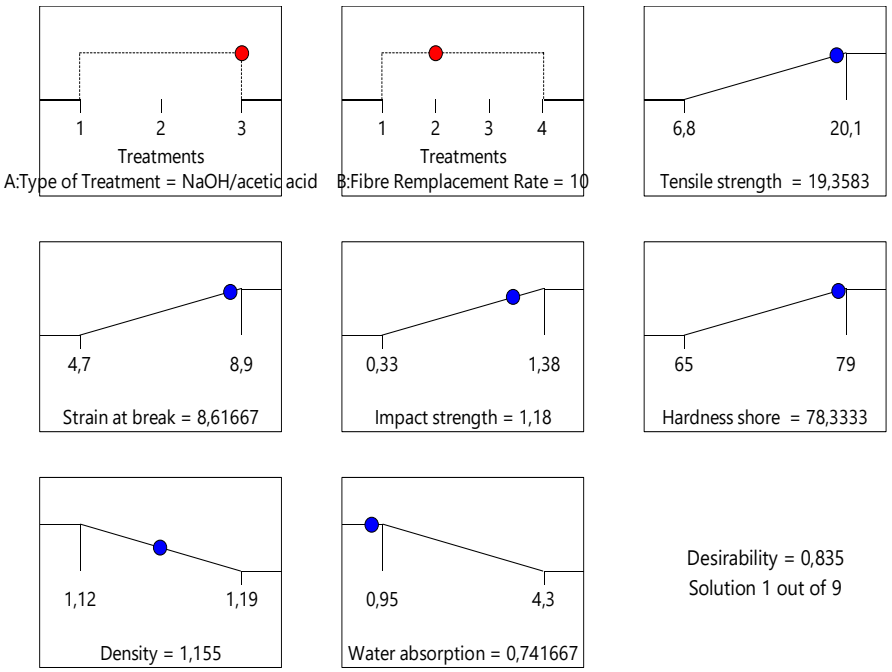

Figure 14: Optimized solutions with a desirability of 0.835.

5 Conclusions

In this study, bio-composites based on unsaturated polyester resin (UPR) reinforced with luffa fibers (LF) were developed using untreated fibers, NaOH-treated fibers, and fibers subjected to a combined NaOH + CH_3COOH treatment. The main conclusions can be summarised as follows:

- FTIR analysis revealed clear interactions between the LF and the UPR matrix, confirming that chemical surface treatment improved fiber-matrix compatibility.
- The combined NaOH + CH_3COOH treatment gave the best overall mechanical performance, with increases of 74% in tensile strength, 192% in impact resistance, and 16.2% in hardness compared with composites reinforced with untreated LF.

- SEM observations highlighted a cleaner and rougher fiber surface after treatment, indicating that the removal of waxy layers and other impurities promoted stronger interfacial adhesion.
- The combined treatment reduced the density of the bio-composites, leading to lighter materials with a more favourable strength-to-weight ratio.
- Water absorption decreased after chemical treatment, especially in the case of the combined process, as a result of lower fiber hydrophilicity and better interfacial compatibility.
- Chemical treatment improved both the mechanical behavior and the durability of the bio-composites, suggesting that these materials could serve as more sustainable and cost-effective alternatives to conventional composites reinforced with glass or carbon fibers.
- The application of a full factorial design combined with response surface methodology proved to be an effective and reliable approach for modeling and predicting the behavior of UPR/LF composites. The high coefficient of determination ($R^2 > 0.90$) and the high concordance between the predicted and experimental values confirm the robustness and accuracy of the developed regression models, thus demonstrating their relevance for the multiparametric optimization of the developed composites.
- The results clearly demonstrate that the combined treatment with NaOH and acetic acid, combined with an optimal fiber replacement rate (10% by weight), enhances interfacial adhesion, resulting in improved mechanical performance while reducing water absorption and density.

The findings demonstrate that luffa fibers (LF), being an abundant and naturally sourced material, are highly promising for producing eco-friendly, low-density bio-composites suitable for structural strengthening and load-bearing uses. Subsequent studies will explore the application of LF-reinforced unsaturated polyester resin systems for structural enhancement purposes.

While the present study demonstrates the beneficial effect of chemical treatments on the interfacial adhesion and short-term mechanical performance of UPR/LF composites, further investigations are required to fully assess their suitability for structural applications. In particular, future work will focus on the long-term durability of these composites under realistic service conditions, including hygrothermal aging, temperature-dependent behaviour, and moisture diffusion over extended periods. Additionally, time-dependent mechanical responses such as creep, stress relaxation, and fatigue performance under cyclic loading will be systematically evaluated. These studies will provide a more comprehensive understanding of material reliability and lifetime performance and contribute to validating the use of luffa fiber-reinforced UPR composites in demanding engineering applications.

Acknowledgement: Not applicable.

Funding Statement: This work was supported by the Deanship of Scientific Research, Vice Presidency for Graduate Studies and Scientific Research, King Faisal University, Saudi Arabia [Grant No. KFU263227].

Author Contributions: The authors confirm contribution to the paper as follows: Conceptualization, Ouided Dehas, Yasmina Biskri, Laidi Babouri, S. M. Anas, Osama Khan, Mohammed Benzerara, Aboulkacem Moutie Hamed and Fouad Boukhelf; methodology, Ouided Dehas, Yasmina Biskri and Laidi Babouri; software, Ouided Dehas; validation, Ouided Dehas, Yasmina Biskri and Laidi Babouri; formal analysis, Ouided Dehas and Yasmina Biskri; investigation, Ouided Dehas; resources, Aboulkacem Moutie Hamed and Fouad Boukhelf; data curation, Ouided Dehas; writing-original draft preparation, Ouided Dehas, Yasmina Biskri, Laidi Babouri, S. M. Anas, Osama Khan, Mohammed Benzerara, Aboulkacem Moutie Hamed and Fouad Boukhelf; writing-review and editing, Yasmina Biskri, Laidi Babouri and Fouad Boukhelf; visualization, Ouided Dehas; supervision, Yasmina Biskri, Laidi Babouri, Mohammed Benzerara and Fouad Boukhelf; project administration, Mohammed Benzerara; funding acquisition, Osama Khan. All authors reviewed and approved the final version of the manuscript.

Availability of Data and Materials: The data that support the findings of this study are available from the Corresponding Author upon reasonable request.

Ethics Approval: Not applicable.

Conflicts of Interest: The authors declare no conflicts of interest.

References

1. Kalangi C, Prabu DA, Jose AS, Jani SP. Experimental characterization of banana fiber reinforced polyester composites. Mater Today Proc. 2022;60:2236–9. [CrossRef].
2. Muktha K, Keerthi Gowda BS. Investigation of water absorption and fire resistance of untreated banana fibre reinforced polyester composites. Mater Today Proc. 2017;4(8):8307–12. [CrossRef].
3. Choudhary S, Kumar Sain M, Kumar V, Saraswat P, Kumar Jindal M. Advantages and applications of sisal fiber reinforced hybrid polymer composites in automobiles: A literature review. Mater Today Proc. 2026;118:105–9. [CrossRef].
4. Akhyar, Gani A, Ibrahim M, Ulmi F, Farhan A. The influence of different fiber sizes on the flexural strength of natural fiber-reinforced polymer composites. Results Mater. 2024;21:100534. [CrossRef].
5. Kareem A, Venkat Reddy P, Snehith Kumar V, Buddi T. Influence of the stacking on mechanical and physical properties of jute/banana natural fiber reinforced polymer matrix composite. Mater Today Proc. 2023. [CrossRef].
6. Koppula SB, Karachi S, Vijaya Kumar P, Borra ND, Phaneendra Y, Neigapula VSN, et al. Investigation into the mechanical characteristics of natural fiber-reinforced polymer composites: Effects of flax and e-glass reinforcement and stacking configuration. Mater Today Proc. 2024;115:82–8. [CrossRef].
7. Jasmin NM, Sathish S, Senthil TS, Naidu BA, Das AD, Arun KK, et al. Investigation on natural fiber reinforced polymer matrix composite. Mater Today Proc. 2023;74:60–3. [CrossRef].
8. Bhowmik R, Das S, Mallick D, Gautam SS. Predicting the elastic properties of hemp fiber—A comparative study on different polymer composite. Mater Today Proc. 2022;50:2510–4. [CrossRef].
9. Condassamy O. Valorisation d'une lignine alcaline industrielle: Vers le développement de nouveaux synthons et oligomères bio-sourcés *Issus* de la lignine [dissertation]. Bordeaux, France: Université de Bordeaux; 2015. (In French)
10. El-Abbassi FE, Assarar M, Ayad R, Bourmaud A, Baley C. A review on Alfa fibre (*Stipa tenacissima* L.): From the plant architecture to the reinforcement of polymer composites. Compos Part A Appl Sci Manuf. 2020;128:105677. [CrossRef].
11. Saheb DN, Jog JP. Natural fiber polymer composites: A review. Adv Polym Technol. 1999;18(4):351–63. [CrossRef].
12. Li X, Tabil LG, Panigrahi S. Chemical treatments of natural fiber for use in natural fiber-reinforced composites: A review. J Polym Environ. 2007;15(1):25–33. [CrossRef].
13. Radzi FSM, Suriani MJ, Abu Bakar A, Khalina A, Ruzaidi CM, Nik WW, et al. Effect of reinforcement of Alkaline-treated sugar palm/bamboo/kenaf and fibreglass/Kevlar with polyester hybrid biocomposites: Mechanical, morphological, and water absorption properties. J Mater Res Technol. 2023;24:4190–202. [CrossRef].
14. Kelkar AD, Mohan R, Bolick R, Shendokar S. Effect of nanoparticles and nanofibers on Mode I fracture toughness of fiber glass reinforced polymeric matrix composites. Mater Sci Eng B. 2010;168(1–3):85–9. [CrossRef].
15. Zhang X, Li W, Shao LH, Li Y, Wang J. Micromechanics-based modeling of temperature-dependent effective moduli of fiber reinforced polymer composites with interfacial debonding. Compos Part A Appl Sci Manuf. 2024;180:108049. [CrossRef].
16. Wang C, Guo L, Xia Y, Zhang C, Sang X, Xu C, et al. Flexural performance and damage evolution of multiple fiberglass-reinforced UV-CIPP composite materials—A view from mechanics and energy release. J Mater Res Technol. 2024;29:3317–39. [CrossRef].
17. Sever K, Sarikanat M, Seki Y, Erkan G, Erdoğan ÜH, Erden S. Surface treatments of jute fabric: The influence of surface characteristics on jute fabrics and mechanical properties of jute/polyester composites. Ind Crops Prod. 2012;35(1):22–30. [CrossRef].

18. Turaka S, Chintalapudi R, Kannaiyan Geetha N, Pappula B, Makgato S. Experimental and numerical analysis of the Microstructure and mechanical properties of unidirectional glass fiber reinforced epoxy composites. Compos Struct. 2024;331:117887. [CrossRef].
19. Tong L, Wang X, Tong J, Yi X, Liu X, Rudd C. Re-use of jute fiber hybrid nonwoven breather within laminated composite applications: A case study. Sustain Mater Technol. 2023;36:e00621. [CrossRef].
20. Chruściel JJ, Leśniak E. Modification of epoxy resins with functional silanes, polysiloxanes, silsesquioxanes, silica and silicates. Prog Polym Sci. 2015;41:67–121. [CrossRef].
21. Park G, Cho NK, Lee Y, Kim CS. Comprehensive parametric analyses on the mechanical performance of 3D printed continuous carbon fibre reinforced plastic. Compos Struct. 2024;329:117804. [CrossRef].
22. Mohammed M, Jawad AJM, Mohammed AM, Oleiwi JK, Adam T, Osman AF, et al. Challenges and advancement in water absorption of natural fiber-reinforced polymer composites. Polym Test. 2023;124:108083. [CrossRef].
23. Demir TN, Yuksel Yilmaz AN, Celik Bedeloglu A. Investigation of mechanical properties of aluminum–glass fiber-reinforced polyester composite joints bonded with structural epoxy adhesives reinforced with silicon dioxide and graphene oxide particles. Int J Adhes Adhes. 2023;126:103481. [CrossRef].
24. Mahesha CR, Shivarudraiah, Mohan N, Suprabha R. Three body abrasive wear studies on nanoclay/NanoTiO_2 filled basalt-epoxy composites. Mater Today Proc. 2017;4(2):3979–86. [CrossRef].
25. Bhat AR, Kumar R, Mural PKS. Natural fiber reinforced polymer composites: A comprehensive review of Tribo-Mechanical properties. Tribol Int. 2023;189:108978. [CrossRef].
26. Hu S, Han P, Meng C, Yu Y, Han S, Wang H, et al. Comparative study of different bonding interactions on the interfacial adhesion and mechanical properties of MXene-decorated carbon fiber/epoxy resin composites. Compos Sci Technol. 2024;245:110352. [CrossRef].
27. Shanmugam D, Thiruchitrambalam M. Static and dynamic mechanical properties of alkali treated unidirectional continuous Palmyra Palm Leaf Stalk Fiber/jute fiber reinforced hybrid polyester composites. Mater Des. 2013;50:533–42. [CrossRef].
28. Parameswaranpillai J, Gopi JA, Radoor S, C. D. MD, Krishnasamy S, Deshmukh K, et al. Turning waste plant fibers into advanced plant fiber reinforced polymer composites: A comprehensive review. Compos Part C Open Access. 2023;10:100333. [CrossRef].
29. Singh MK, Tewari R, Zafar S, Rangappa SM, Siengchin S. A comprehensive review of various factors for application feasibility of natural fiber-reinforced polymer composites. Results Mater. 2023;17:100355. [CrossRef].
30. Elfaleh I, Abbassi F, Habibi M, Ahmad F, Guedri M, Nasri M, et al. A comprehensive review of natural fibers and their composites: An eco-friendly alternative to conventional materials. Results Eng. 2023;19:101271. [CrossRef].
31. Kumar S, Varadarajan YS, Shamprasad MS. Three-body abrasive wear behavior of rice straw fibers reinforced PLA composites. Mater Today Proc. 2023;92:322–6. [CrossRef].
32. Asyraf MRM, Ishak MR, Syamsir A, Nurazzi NM, Sabaruddin FA, Shazleen SS, et al. Mechanical properties of oil palm fibre-reinforced polymer composites: A review. J Mater Res Technol. 2022;17:33–65. [CrossRef].
33. Ezeamaku UL, Onukwuli OD, Ezeh ME, Eze IO, Odimegwu NE, Agu CP. Experimental investigation on influence of selected chemical treatment on banana fibre. Ind Crops Prod. 2022;185:115135. [CrossRef].
34. Balaji R, Raja S, Jeevanandam P, Kailasavalli S, Kaarthik M, Pitchandi P. Study of abrasive water jet machining (AWJM) of coir/banana epoxy composites by adding of fly ash fillers. Mater Today Proc. 2023. [CrossRef].
35. Harle SM. Durability and long-term performance of fiber reinforced polymer (FRP) composites: A review. Structures. 2024;60:105881. [CrossRef].
36. Yaw Attahu C, Ket Thein C, Wong KH, Yang J. Enhanced damping and stiffness trade-off of composite laminates interleaved with recycled carbon fiber and short virgin aramid fiber non-woven mats. Compos Struct. 2022;297:115981. [CrossRef].
37. Baghloul R, Babouri L, Hebhoub H, Boukhelf F, El Mendili Y. Assessment of mechanical behavior and microstructure of unsaturated polyester resin composites reinforced with recycled marble waste. Buildings. 2024;14(12):3877. [CrossRef].
38. Dehas O, Babouri L, Biskri Y, Bardeau JF. Mechanical and morphological properties of unsaturated polyester resin composites reinforced with recycled PET fibers of varying lengths. World J Eng. 2024;21(6):1142–53. [CrossRef].
39. Kamran MJ, Jayamani E, Heng SK, Wong YC. A review: Surface treatments, production techniques, mechanical properties and characteristics of *Luffa cylindrica* bio composites. J Ind Text. 2022;51:215S–45S. [CrossRef].

40. Sangamesh R, Hiremath S, Biradar S, Kumar BS, Sondar P, Vishwanatha HM. Effect of alkaline treatment on mechanical properties of natural fiber-reinforced composite. J Mech Sci Technol. 2024;38(12):6597–605. [CrossRef].
41. Kamran MJ, Jayamani E, Heng SK, Wong YC, Rahman MR, Al-Bogami AS, et al. Characterization and comparative study on chemically treated Luffa fiber as reinforcement for polylactic acid bio-composites. BioResources. 2022;17(2):2576–97. [CrossRef].
42. Boynard CA, Monteiro SN, D'Almeida JRM. Aspects of alkali treatment of sponge gourd (*Luffa cylindrica*) fibers on the flexural properties of polyester matrix composites. J Appl Polym Sci. 2003;87(12):1927–32. [CrossRef].
43. Tanobe V, Flores-Sahagun T, Amico S, Muniz G, Satyanarayana K. Sponge gourd (*Luffa cylindrica*) reinforced polyester composites: Preparation and properties. Def Sci J. 2014;64(3):273–80. [CrossRef].
44. Mohanta N, Acharya SK. Fiber surface treatment: Its effect on structural, thermal, and mechanical properties of *Luffa cylindrica* fiber and its composite. J Compos Mater. 2016;50(22):3117–31. [CrossRef].
45. Shahid AT, Silvestre JD, Hofmann M, Garrido M, Correia JR. Life cycle assessment of an innovative bio-based unsaturated polyester resin and its use in glass fibre reinforced bio-composites produced by vacuum infusion. J Clean Prod. 2024;441:140906. [CrossRef].
46. Mohammad Shohel S, Hossain Riyad S, All Noman A. Study to analyze the mechanical strength of composite glass fiber laminated with resin epoxy, resin polyester, and PVC foam under tensile loading conditions by numerically using finite element analysis via Ansys. Mater Today Proc. 2023. [CrossRef].
47. Indra Reddy M, Prasad Varma UR, Ajit Kumar I, Manikanth V, Kumar Raju PV. Comparative evaluation on mechanical properties of jute, pineapple leaf fiber and glass fiber reinforced composites with polyester and epoxy resin matrices. Mater Today Proc. 2018;5(2):5649–54. [CrossRef].
48. Pihtili H. An experimental investigation of wear of glass fibre–epoxy resin and glass fibre–polyester resin composite materials. Eur Polym J. 2009;45(1):149–54. [CrossRef].
49. Pıhtılı H, Tosun N. Investigation of the wear behaviour of a glass-fibre-reinforced composite and plain polyester resin. Compos Sci Technol. 2002;62(3):367–70. [CrossRef].
50. Ghali L, Msahli S, Zidi M, Sakli F. Effects of fiber weight ratio, structure and fiber modification onto flexural properties of *Luffa*-polyester composites. Adv Mater Phys Chem. 2011;1(3):78–85. [CrossRef].
51. Siqueira J, Botaro VR. *Luffa cylindrica* fibres/vinylester matrix composites: Effects of 1, 2, 4, 5-benzenetetracarboxylic dianhydride surface modification of the fibres and aluminum hydroxide addition on the properties of the composites. Compos Sci Technol. 2013;82:76–83. [CrossRef].
52. Tanobe VOA, Sydenstricker THD, Munaro M, Amico SC. A comprehensive characterization of chemically treated Brazilian sponge-gourds (*Luffa cylindrica*). Polym Test. 2005;24(4):474–82. [CrossRef].
53. Ghali L, Msahli S, Zidi M, Sakli F. Effect of pre-treatment of *Luffa* fibres on the structural properties. Mater Lett. 2009;63(1):61–3. [CrossRef].
54. Boynard CA, D'Almeida JRM. Morphological characterization and mechanical behavior of sponge gourd (*Luffa cylindrica*)–polyester composite materials. Polym Plast Technol Eng. 2000;39(3):489–99. [CrossRef].
55. Sarikaya E, Çallioğlu H, Demirel H. Production of epoxy composites reinforced by different natural fibers and their mechanical properties. Compos Part B Eng. 2019;167:461–6. [CrossRef].
56. Baley C. Fibres naturelles de renfort pour matériaux composites. Paris, France: Techniques de l'Ingénieur; 2013. [CrossRef].
57. Haghdan S, Smith GD. Natural fiber reinforced polyester composites: A literature review. J Reinf Plast Compos. 2015;34(14):1179–90. [CrossRef].
58. Alhijazi M, Safaei B, Zeeshan Q, Asmael M, Eyvazian A, Qin Z. Recent developments in *Luffa* Natural fiber composites: Review. Sustainability. 2020;12(18):7683. [CrossRef].
59. ASTM D303/D3039M-14. Test method for tensile properties of polymer matrix composite materials. West Conshohocken, PA, USA: ASTM International; 2025. [CrossRef].
60. ASTM D256-24. Standard test methods for determining the izod pendulum impact resistance of plastics. West Conshohocken, PA, USA: American Society for Testing and Materials; 2024.
61. ASTM D2240-15. Standard test method for rubber property—Durometer hardness. West Conshohocken, PA, USA: ASTM International; 2021. [CrossRef].

62. ISO 1183-1:2019. Plastics—Methods for determining the density of non-cellular plastics—Part 1: Immersion method, liquid pyknometer method and titration method. Geneva, Switzerland: International Organization for Standardization (ISO); 2019.
63. ASTM D5229/D5229M-20. Standard test method for moisture absorption properties and equilibrium conditioning of polymer matrix composite materials. West Conshohocken, PA, USA: ASTM International; 2020.
64. Biskri Y, Babouri L, Boukhelf F, Charradi K, Annaba K, El Mendili Y. On the physical-mechanical behavior of fiber cement composite: Effect of chemical treatment of sisal fibers. J Build Eng. 2025;101:111978. [CrossRef].
65. John MJ, Molaba TP. Mechanical properties and water sorption of chemically modified natural fiber-based composites. In: Encyclopedia of materials: Composites. Amsterdam, The Netherlands: Elsevier; 2021. p. 159–67. [CrossRef].
66. Samanth M, Bhat KS. Conventional and unconventional chemical treatment methods of natural fibres for sustainable biocomposites. Sustain Chem Clim Action. 2023;3:100034. [CrossRef].
67. Ghali L, Aloui M, Zidi M, Bendaly H, M'sahli S, Sakli F. Effect of chemical modification of *Luffa cylindrica* fibers on the mechanical and hygrothermal behaviours of polyester/*Luffa* composites. BioResources. 2011;6(4):3836–49. [CrossRef].
68. Yang Y, Zhang H, Liu X, Deng Y, Sun M, Wang J, et al. Hierarchical interface design of jute fibers/polypropylene composites for enhanced interfacial and mechanical properties. J Clean Prod. 2024;450:141966. [CrossRef].
69. Sun Y, Chen Q, Zhang X, Ma Y, Wu Y, Guo Z, et al. Gypsum reinforced using hemp fibers: Enhanced interfacial compatibility by dual-modification strategy. Constr Build Mater. 2024;419:135521. [CrossRef].
70. Sathishkumar G, Uma Devi A, Prem Kumar Reddy M, Kanthe VN, Palaniswamy D, Kalyana Chakravarthy PR, et al. Experimental study on mechanical performance and microstructural characterization of optimized sisal fiber reinforced polyester composites. Sci Rep. 2025;15:36348. [CrossRef].
71. Hasibul Hasan M, Biswas S, Abdus Sabur M, Shafiur Rahman GM, Al Mamun MA. Green biocomposites from agro-waste with central layer architecture: a performance comparison against glass fiber composite. Adv Polym Technol. 2026;2026:3572010. [CrossRef].
72. Ramachandran A, Mavinkere Rangappa S, Kushvaha V, Khan A, Seingchin S, Dhakal HN. Modification of Fibers and matrices in natural fiber reinforced polymer composites: a comprehensive review. Macromol Rapid Commun. 2022;43:2100862. [CrossRef].
73. Kalusuraman G, Siva I, Winowlin Jappes JT, Gao XZ, Amico SC. Fibre loading effects on dynamic mechanical properties of compression moulded luffa fibre polyester composites. Int J Comput Aided Eng Technol. 2018;10:157–65. [CrossRef].
74. Kalusuraman G, Siva I, Munde Y, Selvan CP, Anand Kumar S, Amico SC. Dynamic-mechanical properties as a function of luffa fibre content and adhesion in a polyester composite. Polym Test. 2020;87:106538. [CrossRef].
75. Derdour D, Behim M, Benzerara M. Effect of date palm and polypropylene fibers on the characteristics of self-compacting concretes: Comparative study. Frat Ed Integrità Strutt. 2023;17(64):31–50. [CrossRef].
76. Benzerara M, Guihéneuf S, Belouettar R, Perrot A. Combined and synergic effect of Algerian natural fibres and biopolymers on the reinforcement of extruded raw earth. Constr Build Mater. 2021;289:123211. [CrossRef].
77. Kersenna S, Hammouda A, Anas SM, Biskri Y, Babouri L, Saidani M, et al. Surface treatment of Alfa fibers to improve mechanical performance and matrix compatibility in sustainable bio-composites. Innov Infrastruct Solut. 2025;10(11):492. [CrossRef].
78. Villaça JC, da Silva LCRP, Locatelli FR, Meireles PW, do Carmo FA, Rodrigues CR, et al. Full-factorial design for statistical planning of attritor milling parameters and evaluation of effects on particle size and structure of sodium-montmorillonite. Eng Res Express. 2020;2(1):015050. [CrossRef].
79. Zahid M, Shafiq N, Isa MH, Gil L. Statistical modeling and mix design optimization of fly ash based engineered geopolymer composite using response surface methodology. J Clean Prod. 2018;194:483–98. [CrossRef].
80. Abdellatief M, Elrahman MA, Elgendy G, Bassioni G, Tahwia AM. Response surface methodology-based modelling and optimization of sustainable UHPC containing ultrafine fly ash and metakaolin. Constr Build Mater. 2023;388:131696. [CrossRef].

81. El Moustapha B, Boukhelf F, Gascoin S, Larose X, Khadraoui F, Chateigner D. Enhancing recycled aggregate-based geopolymer concrete: The effect of metakaolin on performance and microstructure. Open Ceram. 2026;25:100931. [CrossRef].
82. Khan MI. Robust prediction models for flow and compressive strength of sustainable cement grouts for grouted macadam pavement using RSM. Constr Build Mater. 2024;448:138205. [CrossRef].